Journal of Medicinal Chemistry

Article

pubs.acs.org/jmc

6-OH-Phenanthroquinolizidine Alkaloid and Its Derivatives Exert Potent Anticancer Activity by Delaying S Phase Progression

Yuxiu Liu,[†,§] Lihua Qing,[‡,§] Chuisong Meng,[†,§] Jiajie Shi,[‡,§] Yan Yang,[‡] Ziwen Wang,[†] Guifang Han,[†] Yi Wang,[‡] Jian Ding,[‡] Ling-hua Meng,[*,‡] and Qingmin Wang[*,†]

[†]State Key Laboratory of Elemento-Organic Chemistry, Research Institute of Elemento-Organic Chemistry, Nankai University, Tianjin 300071, P. R. China

[‡]Division of Anti-Tumor Pharmacology, State Key Laboratory of Drug Research, Shanghai Institute of Materia Medica, Chinese Academy of Sciences, Shanghai 201203, P. R. China

Supporting Information

ABSTRACT: To discover new phenanthroindolizidine and phenanthroquinolizidine alkaloids as potential anticancer drug candidates, non-natural 6-*O*-desmethylcryptopleurine (**2**) and its derivatives were prepared. Most of the new compounds exhibited potent antiproliferative activity against A549 and BEL-7402 cells, with the lowest IC_{50} being 3 nM. Optically pure **2-R** was further evaluated against a panel of 30 cancer cell lines and found to inhibit the proliferation of all tested cell lines, including three multidrug-resistant cell lines, with an average IC_{50} value of 2.1 nM, which is much lower than that of previously reported phenanthroindolizidine DCB-3503 (**1**, IC_{50}: 166.7 nM). A mechanistic evaluation showed that **2-R** potently inhibited cell growth and colony formation, which are associated with a delay in S phase progression through the inhibition of DNA synthesis. These results along with further study on the safety profile of these compounds will facilitate the discovery of new phenanthroindolizidine and phenanthroquinolizidine alkaloids for use as anticancer drug candidates.

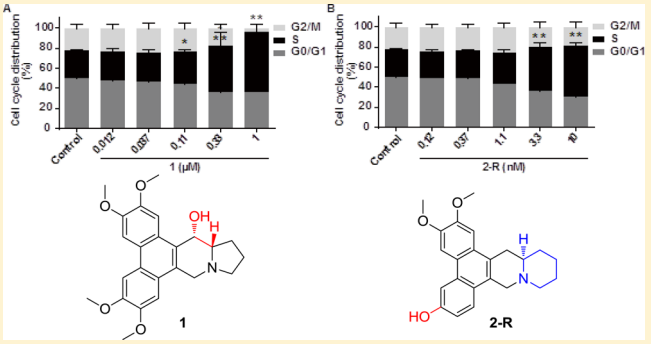

INTRODUCTION

Naturally occurring compounds and their derivatives are important constituents for cancer therapy or prevention. Much effort has been drawn to the discovery of new drug candidates from natural compounds due to their diversified structures and distinct mechanisms of action. Tylophorine (Figure 1) is a phenanthroindolizidine alkaloid that was first separated from *Tylophora indica* in 1935.[1] Tylophorine and its analogues have drawn great interest from academia and industry due to their unique chemical structures and remarkable biological activities. In the 1960s, tylocrebrine entered phase I clinical trials as an anticancer drug candidate,[2] but the trial was terminated due to its undesirable central nervous system side effects.[3] Tyloindicine F (NSC-650393) and tyloindicine G (NSC-650394) were reported to exhibit potent activity in a NCI-60 screen (NCI, DTP), with an average GI_{50} value of 0.1 nM.[4] A number of analogues were then discovered that displayed significant activity against a wide variety of tumor cell lines.[5−11] DCB-3503 (NSC-716802, **1**), a synthetic analogue, was also reported to inhibit the proliferation of multidrug-resistant cells, including KB-V1, KB-MDR, KB-7D, and KB-HU-R, with an average GI_{50} value of around 30 nM.[5] Phenanthroquinolizidine alkaloids, represented by cryptopleurine, are structural analogues of phenanthroindolizines and have shown more potent anticancer activity[9,12] than phenanthroindolizines.

Various biological mechanisms have been proposed to explain the antitumor activities of these alkaloids, but the exact target(s) and the mechanisms of action have not yet been clearly established. Tylocrebrine was reported to inhibit protein synthesis in Ehrlich ascites-tumor cells[13] and to inhibit DNA and RNA syntheses in HeLa cells.[14] Phenanthroindolizidine alkaloids pergularinine and tylophorinidine were found to exert their activities by inhibiting thymidylate synthase[15] and dihydrofolate reductase.[16] More recently, Chen et al. discovered that *S*-(1)-deoxytylophorinidine intercalates nucleic acids.[17] Furthermore, a phenanthroindolizidine alkaloid was found to inhibit protein synthesis in a cell-free translation assay.[18] These alkaloids also displayed potent regulatory activity on cell cycle progression,[5] which might be associated with a downregulation of cyclin D1.[6,19] In addition, it was demonstrated that these alkaloids inhibited the transcriptional activities mediated by key transcription factors such as activator protein-1 (AP1),[5,20] nuclear factor-kappa B (NF-κB),[5,6] and hypoxia inducible factor-1 (HIF1).[21] Previous structure−activity relationship studies indicated that changes in their structures would not

Received: October 30, 2016

DOI: 10.1021/acs.jmedchem.6b01502
J. Med. Chem. XXXX, XXX, XXX−XXX

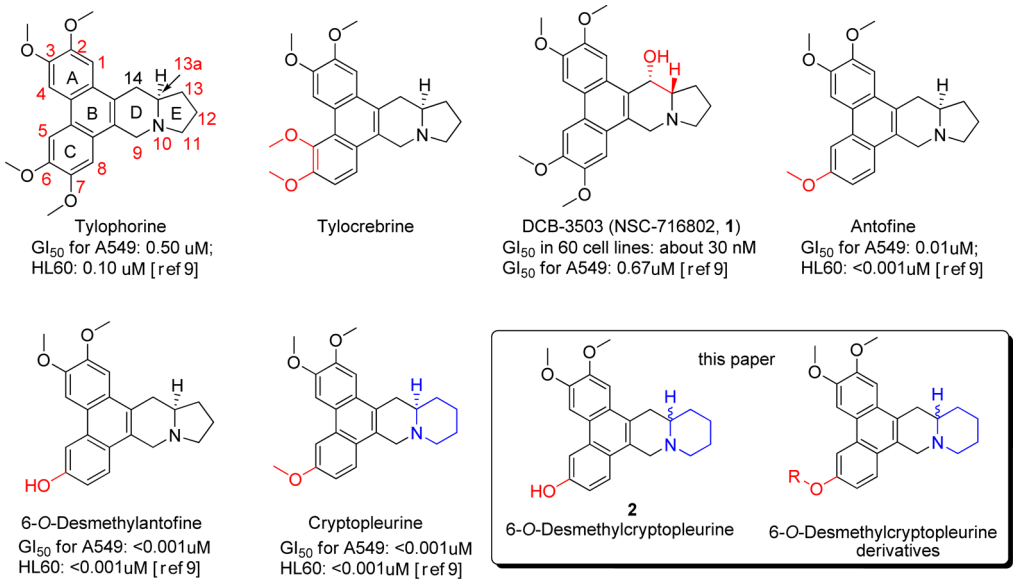

Figure 1. Representative phenanthroindolizidines and phenanthroquinolizidines with anticancer activity.

Scheme 1. Synthetic Route for 6-*O*-Desmethylcryptopleurine 2[a]

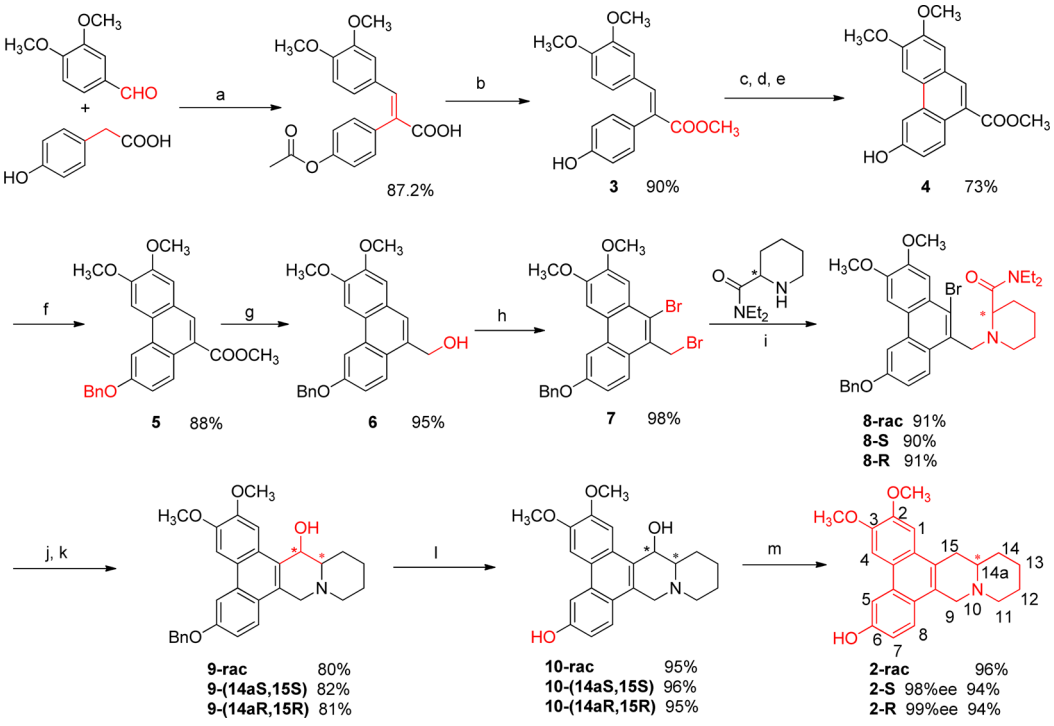

[a]Reagents and conditions: (a) Ac_2O, Et_3N, reflux; (b) CH_3OH, H_2SO_4,reflux; (c) MnO_2, CF_3COOH, rt; (d) Ac_2O, 40 °C; (e) H_2O, 70 °C; (f) BnBr, K_2CO_3, acetone, reflux; (g) $LiAlH_4$, THF, reflux; (h) Br_2, $CHCl_3$, rt; (i) K_2CO_3, DMF, reflux; (j) tetramethylethylenediamine, *n*-BuLi, THF, −78 °C; (k) CH_3OH, $NaBH_4$, − 40 °C, then rt; (l) H_2, Pd/C, THF/CH_3OH, rt; (m) Et_3SiH, CF_3COOH, rt.

only result in changes in the potency of their activities but also alter the targets of their actions.[12,22] Therefore, to find new potent analogues and explore their mechanisms of action, it is important to identify new druggable compounds.

It was reported that 6-*O*-desmethylantofine exhibited more potent anticancer activity than antofine.[9] The group at the 6-position of the phenanthrene ring might have a non-negligible role on the activity. We hypothesized that 6-*O*-desmethylcryptopleurine (**2**, Figure 1) may also possess better anticancer activity than cryptopleurine. In this study, we synthesized 6-*O*-desmethylcryptopleurine, referring to the structure of 6-*O*-desmethylantofine. The esters and ethers of 6-*O*-desmethylcryptopleurine were also prepared to investigate whether changes at this position would enhance its activity. To analyze the structure−activity relationships, we compared the cytotoxicity of all new synthesized compounds as well as **1** against A549 and BEL-7402 cells. Furthermore, the most potent compound was selected to evaluate its anticancer spectrum in vitro and investigate its anticancer mechanism.

DOI: 10.1021/acs.jmedchem.6b01502
J. Med. Chem. XXXX, XXX, XXX−XXX

Scheme 2. Synthetic Route for Ester Derivatives 11−18[a]

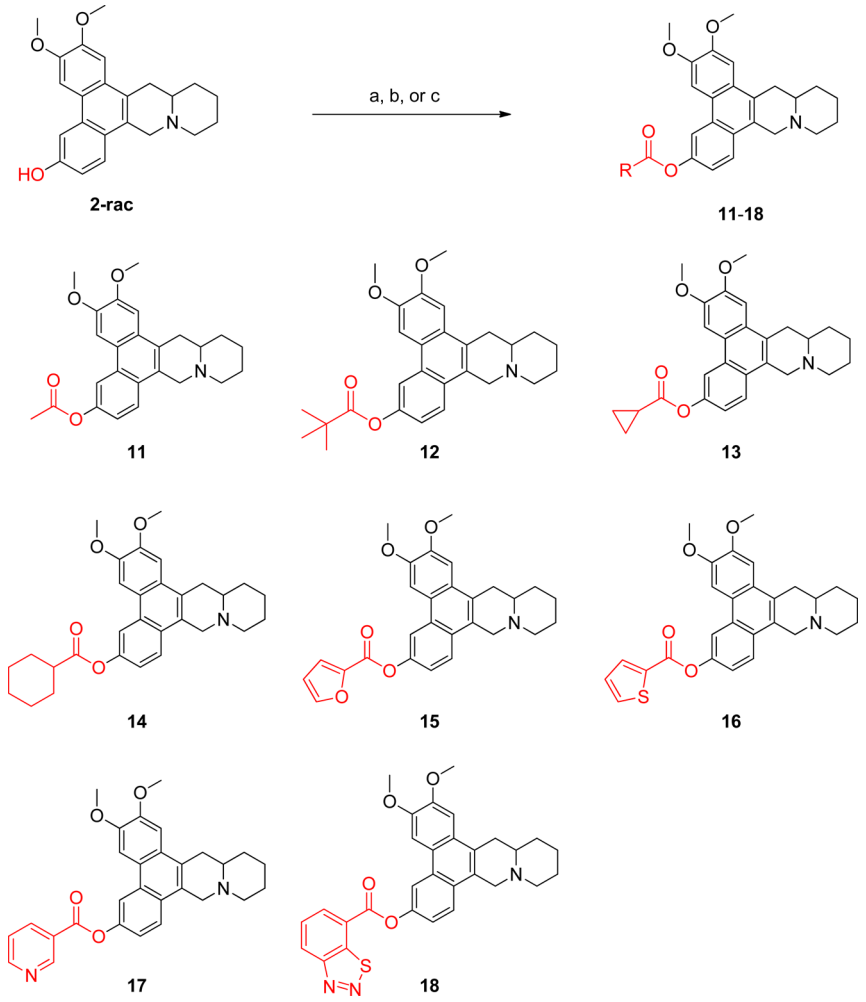

[a]Reagents and conditions: (a) for **11**: Ac_2O, Et_3N, CH_2Cl_2, rt; (b) for **12**: pivaloyl chloride, Et_3N, cat. DMAP, CH_2Cl_2, rt; (c) for **13−18**: RCO_2H, EDCI, Et_3N, cat. DMAP, CH_2Cl_2, rt

RESULTS

Chemistry. We previously reported a synthetic method for **2-rac**.[23] To obtain optically pure compounds of **2** and their derivatives, we designed another route suitable for providing chiral **2-S** and **2-R**[24,25] (Scheme 1) according to the synthetic methods for 6-*O*-desmethylantofine[9] and cryptopleurine.[26] At the beginning, 3,4-dimethoxybenzaldehyde reacted with 4-hydroxyphenylacetic acid to give diaryl propionic acid through a Perkin reaction; after esterification, the resulting **3** was converted to phenanthreneformate **4** through a three-step sequence in one pot, i.e., a MnO_2/CF_3COOH-catalyzed oxidative coupling, an acid-catalyzed rearrangement, and then a hydrolysis reaction. To eliminate the influence of the phenolic hydroxyl group on subsequent reactions, we chose to protect the hydroxyl with a benzyl group and obtained **5**. Next, we reduced the formate to corresponding methanol, which was then treated with bromine to afford a double brominated product, **7**. Compound **7** was allowed to react with racemic or optically pure pipecolamide to form key intermediate **8**, with the chirality well maintained (**8-S** was obtained from L-pipecolamide, **8-R** was from D-pipecolamide, and **8-rac** was from racemic pipecolamide). Compound **8** was treated with *n*-butyl lithium at −78 °C, and the generated carbon ion attacked the carbonyl in the amide, affording the C15-oxo compound via a Parham cyclization process. Because this compound is not stable, it was not separated but directly reduced by sodium borohydride to form stable C15-hydroxy compound **9**. This step had high stereoselectivity: the C15-hydroxyl and C14a-hydrogen were always in the trans position.[27] After deprotection of the benzyl group by palladium-catalyzed hydrogenation to **10** and two subsequent steps to remove the hydroxyl at C15, final product 2,3-dimethoxy-6-hydroxy-phenanthroquinolizidine (**2-rac**, i.e., 6-*O*-desmethylcryptopleurine) was obtained, with an ee value of **2-S** and **2-R** as high as 98%.

The derivatives of **2-rac** were divided into esters and ethers. The esterification conditions were somewhat different when different acylation reagents were used. When preparing acetate **11**, the reaction used acetic anhydride as the acylation reagent and triethylamine as the deacid agent; when preparing pivalate **12**, pivaloyl chloride was used with triethylamine as the deacid agent and DMAP was used as the catalyst. The syntheses of **13−18** used the corresponding acids as reactants, using (3-(dimethylamino)propyl)ethyl carbodiimide hydrochloride (EDCI) as the dehydrating reagent in the presence of triethylamine and DMAP (Scheme 2).

DOI: 10.1021/acs.jmedchem.6b01502
J. Med. Chem. XXXX, XXX, XXX−XXX

Scheme 3. Synthetic Route for Ether Derivatives 19−22

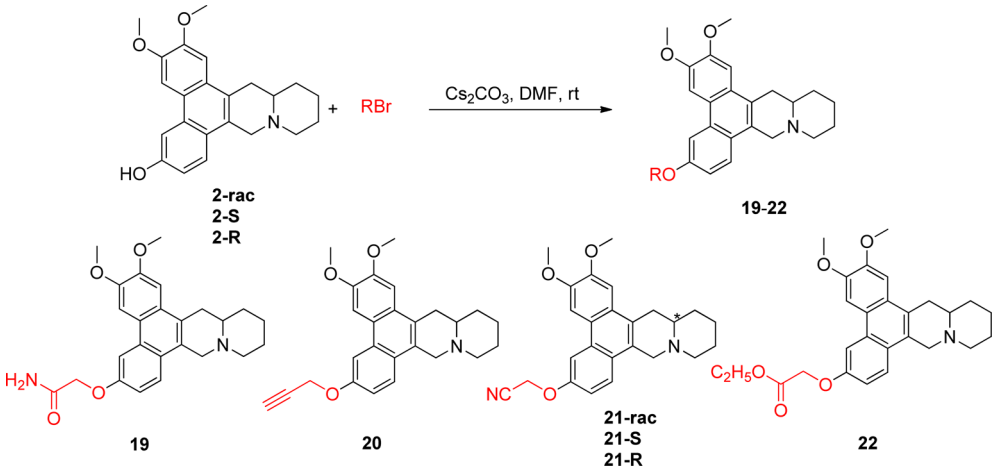

Scheme 4. Synthetic Route for Amino Acid Derivative 25[a]

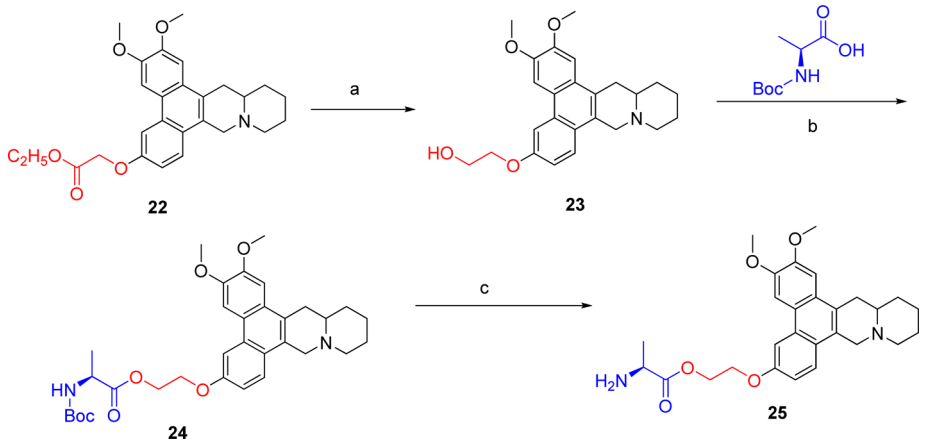

[a]Reagents and conditions: (a) $LiAlH_4$, THF, ice bath, then rt; (b) EDCI, Et_3N, DMAP, CH_2Cl_2, rt; (c) CF_3COOH, CH_2Cl_2, rt.

Etherification derivatives **19−22** were prepared by reacting **2** with a bromide (bromoacetamide, propargyl bromide, bromoacetonitrile, or ethyl bromoacetate) via a nucleophilic substitution reaction in the presence of a base. Using optically pure raw **2-S** and **2-R**, optically pure products **21-S** and **21-R** were obtained, respectively (Scheme 3).

When an amino acid directly connects to the phenol hydroxyl, the resulting ester is found to be unstable and easily undergoes hydrolysis. To introduce an amino acid moiety into the structure of **2**, e.g., compound **25**, we first reduced ester **22** to corresponding alcohol **23**; then, **23** was allowed to react with Boc-protected L-alanine to form **24**, which was further treated with trifluoroacetic acid to remove the Boc group, affording **25** (Scheme 4).

In Vitro Anticancer Activity Screening and Mechanistic Study. *New Phenanthroquinolizidine Alkaloids Possess Potent Activity against the Proliferation of Human Cancer Cells.* To test the anticancer activity of the newly synthesized phenanthroquinolizidine alkaloids, we first investigated their antiproliferative activities against human lung adenocarcinoma A549 cells and human hepatocellular carcinoma BEL-7402 cells. As shown in Table 1, all of the compounds exhibited potent antiproliferative activity against A549 and BEL-7402 cells, with IC_{50} values in the low nanomolar range. Although compound **9-rac** is structurally similar to **1**, **9-rac** (IC_{50} values of 1.534 and 0.917 μM for A549 and BEL-7402 cells, respectively) is somehow less active than **1** (IC_{50} values of 0.283 and 0.110 μM), which suggested that substituents on the phenanthrene ring greatly influence the activity. When the benzyl group on the 6-hydroxy of phenanthroquinolizidine is removed, the resulting compound **10-rac** displayed a remarkably increased activity (IC_{50} values of 12 and 8 nM). Compound **2-rac**, which was generated by further removing the 15-hydroxy group of phenanthroquinolizidine, exhibited remarkable activity, but it was slightly inferior to **10-rac** (IC_{50} values of 19 and 16 nM). Because both **2-rac** and **10-rac** are poorly soluble and **10-rac** is unstable, **2-rac** was chosen as the substrate to make esters or ethers to improve the solubility. Most of the newly synthesized compounds had better solubility and were more potent than **1** (Table 1). For esters **11−18**, the electrical properties and volume of the acyl moiety played an important role. An electron-donating group with a small volume on the carbonyl improved the activity more than an electron-withdrawing group with a large volume. For example, acetate **11**, cyclopropylcarboxylate **13**, and 2-furancarboxylate **15** were more potent than the corresponding pivilate **12**, cyclohexylcarboxylate **14**, and 2-pyridylcarboxylate **17**. Compound **18** could be regarded as an exception as it showed similar activity with a relatively larger volume compared to that of compound **13**. For ethers **19−22** and **25**, most of

DOI: 10.1021/acs.jmedchem.6b01502
J. Med. Chem. XXXX, XXX, XXX−XXX

Table 1. IC_{50} Values of Compounds against the Proliferation of A549 and BEL-7402 Cells[a]

Compound	Structure	A549	BEL-7402
1		0.283±0.146	0.110±0.012
9-rac		1.534±0.434	0.917±0.216
10-rac		0.012±0.003	0.008±0.003
2-rac		0.0029 ± 0.0004	0.0034 ± 0.0002
11	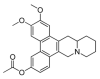	0.022±0.012	0.023±0.022
12	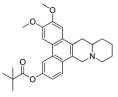	0.103±0.004	0.136±0.081
13		0.030±0.003	0.029±0.009
14	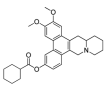	0.191±0.079	0.115±0.001
15	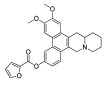	0.052±0.001	0.059±0.043
16	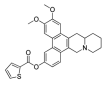	0.115±0.002	0.079±0.018
17	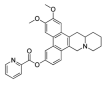	0.277±0.002	0.238±0.116
18	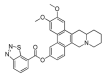	0.029±0.001	0.02±0.013
19	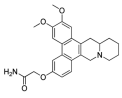	0.016±0.009	0.014±0.013
20	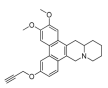	0.030±0.001	0.033±0.012
21-rac	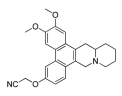	0.003±0.004	0.006±0.005
22	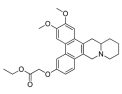	0.458±0.161	0.411±0.177
25	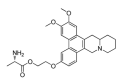	0.049±0.014	0.047±0.025

[a]Values are the mean ± SD (μM).

them displayed superior activity compared to **1**, which may also be due to the small volume of the substituents. Among them, **21-rac** was the most potent compound against both A549 and BEL-7402 cells, with IC_{50} values of 3 and 6 nM, respectively.

Because compounds **2** and **21** displayed potent antiproliferative activity in the pilot screening, we conducted chiral syntheses of **2** and **21** to obtain enantiomerically pure compounds to investigate the influence of the optical configuration on their anticancer activity. As shown in Table 2, both **2-R** and **21-R** were significantly more potent than their S-configuration enantiomers. **2-R** displayed the most potent activity among the compounds tested, with IC_{50} values of 0.7 nM against A549 cells and 1.7 nM against BEL-7402 cells.

Table 2. IC_{50} Values of Compounds against A549 and BEL-7402 Cells[a]

Compound	Structure	A549	BEL-7402
2-rac		1.2±0.2	3.5±0.5
2-S		181.9±78.7	320.1±67.9
2-R		0.7±0.1	1.7±0.7
21-rac		1.0±0.2	2.2±0.8
21-S		12.9±4.5	25.8±5.0
21-R		0.8±0.1	2.4±0.1

[a]Values are the mean ± SD (nM).

Because **2-R** and **21-R** displayed potent antiproliferative activity against lung cancer A549 cells and hepatocellular carcinoma BEL-7402 cells, we next tested the antiproliferative activity of the two compounds against normal lung fibroblast MRC-5 and MRC-9 cells and normal liver LO2 cells. As shown in Table 3, the IC_{50} values of **2-R** and **21-R** obtained against normal MRC-5 or MRC-9 cells are 3−4-fold higher than those obtained against A-549 cells, suggesting that **2-R** and **21-R** might be more potent inhibitors of tumor cell proliferation. Similar results were obtained by comparing the IC_{50} values against normal liver cells and liver cancer cells. The clinical trial of tylocrebrine was terminated due to its undesirable central nervous system side effects. We also evaluated the cytotoxicity of **2-R** and **21-R** against primary neurons. The viability of neurons decreased in a concentration-dependent manner up to 10 nM and remained at a similar level up to 300 nM (Table S1). Both compounds inhibited cell viability by about 50% at 300 nM, indicating that primary neurons tolerate **2-R** and **21-R**.

Since **2-R** was more potent than **21-R** against all tested cell lines, **2-R** was selected for further evaluation and mechanistic study.

***2-R** Exerts Potent Antiproliferative Activity against a Panel of Human Cancer Cell Lines.* The antiproliferative activity of **2-R** was further evaluated in a panel of 30 cancer cell lines including 8 hematoma cell lines, 4 breast cancer cell lines, 3 gastric cancer cell lines, and others. Compound **2-R** displayed potent activity, inhibiting the proliferation of all tested cell lines

DOI: 10.1021/acs.jmedchem.6b01502
J. Med. Chem. XXXX, XXX, XXX−XXX

Table 3. IC_{50} Values of Compounds against the Indicated Cell Lines[a]

compound	A549	MRC-5	MRC-9	BEL-7402	LO2
2-R	0.7 ± 0.1	2.6 ± 0.4	2.2 ± 0.7	1.7 ± 0.7	2.7 ± 1
21-R	0.8 ± 0.1	3.2 ± 0.7	2.7 ± 0.2	2.4 ± 0.1	3.9 ± 1.4

[a]Values are the mean ± SD (nM).

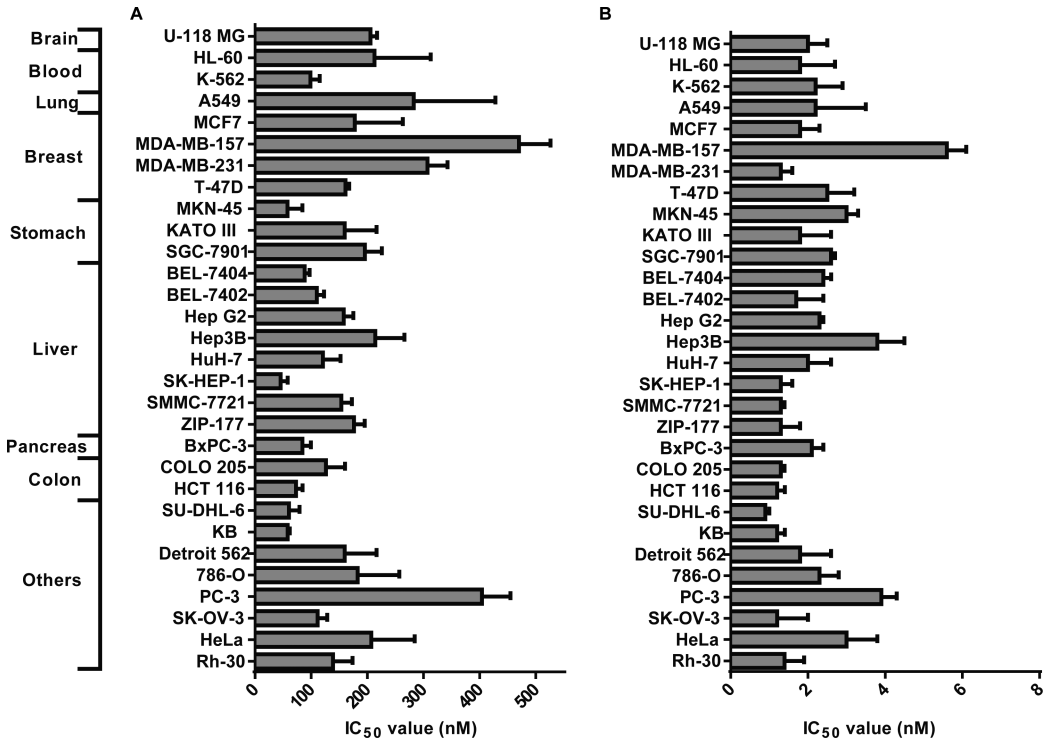

Figure 2. 2-R potently inhibits cell proliferation. Cells seeded in 96-well plates were treated with **1** (A) or **2-R** (B) for 72 h. Cell proliferation of HL-60, K-562, and SU-DHL-6 cells was measured by an MTT assay, and the rest of the cells were tested by an SRB assay. IC_{50} values are depicted. Data shown are the mean ± SD of three independent experiments.

with an average IC_{50} value of 2.1 nM, which is much lower than that of control compound **1** (IC_{50}: 166.7 nM), indicating its superior activity (Figure 2).

To detect the activity of **2-R** and **1** against cell proliferation in a real-time manner, an IncuCyte ZOOM system[28] was utilized to monitor cell proliferation continuously. As shown in Figure 3B, treatment of BEL-7402 cells with different concentrations of **2-R** significantly attenuated cell proliferation, and 3.3 nM **2-R** completely blocked this process up to 10 days. Similar results were obtained in the presence of **1**, but a much higher concentration was required to display a potency similar to that of **2-R** (Figure 3A), further proving that **2-R** is more potent than **1**.

To further evaluate the effect of **2-R** on the clonogenicity of cancer cells, a plate colony formation assay was performed. As shown in Figure 3C,D, the clonogenic ability of BEL-7402 cells decreased in a dose-dependent manner in the presence of **2-R**, and almost no colony was observed upon treatment with 100 nM **2-R**. Similarly, **1** inhibited colony formation, but it did so with much lower potency than **2-R**.

***2-R* Significantly Delays S Phase Progression.** Because **2-R** significantly inhibited cell proliferation, we further explored its mechanism of action by investigating its impact on cell cycle progression. BEL-7402 cells were treated with **2-R** for 24 h, and flow cytometry analysis was performed to detect the cell cycle distribution. As shown in Figure 4, cells in S phase accumulated in a dose-dependent manner upon **2-R** treatment. The population of cells in S phase increased from 27.5 ± 1 to 50.3 ± 3.5% in the presence of 10 nM **2-R**. Similar results were obtained in the presence of **1**, although a much higher concentration was required to induce S phase arrest.

To closely investigate the effect of **2-R** on S phase progression, BEL-7402 cells were synchronized in early S phase by aphidicolin, and cells were then incubated in fresh media with or without the test compounds. As shown in Figure 5A, cells in the vehicle control group entered G2-metaphase 4 h after being released from aphidicolin, whereas most cells remained in S phase at the same time in the presence of **2-R**, indicating that **2-R** treatment slowed the progression from S to G2 phase. Moreover, **2-R** delayed the progression of S phase up to 24 h at 10 nM. Similar results were obtained with **1**, suggesting that both compounds induce S phase arrest by a similar mechanism.

We also confirmed that **2-R** delayed S phase progression in human hepatoma cancer SMMC-7721 and ZIP-177 cells (Figure 5B,C).

***2-R* Inhibits DNA Synthesis without Inducing DNA Damage in BEL-7402 Cells.** We next investigated the mechanism by which **2-R** delays S phase progression. Because DNA replication is an important process during S phase, interruption of DNA synthesis would result in aberrant S phase progression. A BrdU incorporation assay was performed to

DOI: 10.1021/acs.jmedchem.6b01502
J. Med. Chem. XXXX, XXX, XXX−XXX

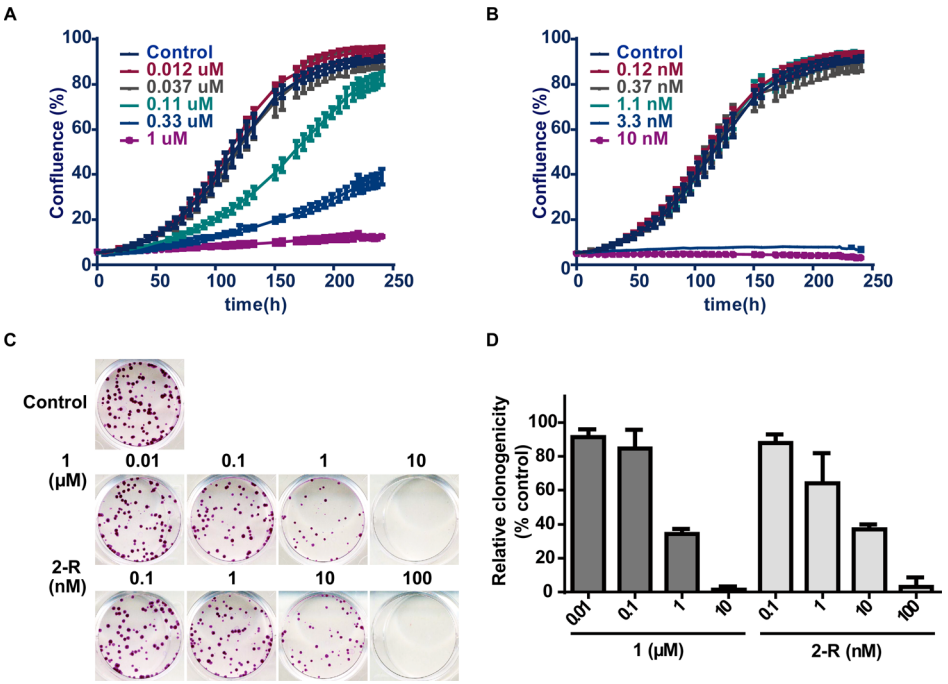

Figure 3. 2-R inhibits cell proliferation and colony formation. (A, B) Representative growth curves of BEL-7402 cells in the presence of various concentrations of **1** (A) or **2-R** (B). (C) Representative images of colony formation. (D) Quantitation of colonies formed in the presence of **1** or **2-R**. Data shown are the mean ± SD of three independent experiments.

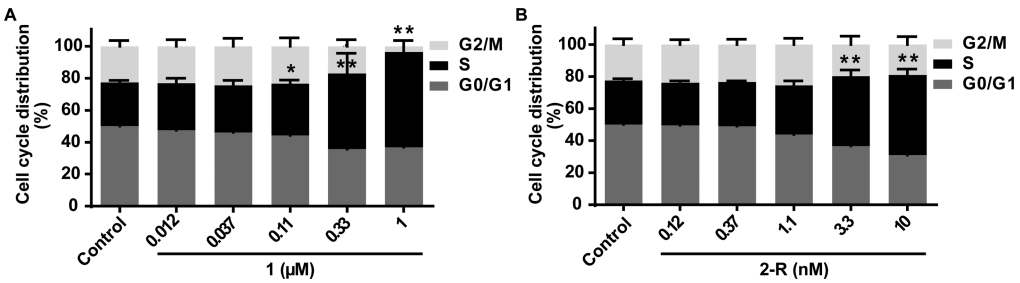

Figure 4. 2-R induces S phase accumulation. BEL-7402 cells were treated with **1** (A) or **2-R** (B) for 24 h, and the cell cycle distribution was detected with flow cytometry. **, $P < 0.01$; *, $P < 0.05$ compared with the population of cells in S phase in the control group.

detect the effect of **2-R** on DNA synthesis. As shown in Figure 6A,B, BrdU-positive cells decreased in a concentration-dependent manner after BEL-7402 cells were treated with **2-R** or **1**, demonstrating the inhibition of DNA synthesis.

DNA single- or double-strand breaks may result in DNA synthesis inhibition. As DNA single-strand breaks transform into double-strand breaks as DNA replication forks progress, we tested the level of phospho-H2AX (γH2AX) as a marker for DNA damage. As shown in Figure 6C, a robust increase in γH2AX, phosphorylated CHK2 at Thr68, and phosphorylated CHK1 at Ser345 was observed after treatment of BEL-7402 cells with CPT (1 μM), which is known to induce DNA damage by trapping the topoisomerase I–DNA complex.[29] However, the level of the tested proteins remained unchanged upon treatment with **2-R** or **1**, even at relative high concentrations, indicating that **2-R** and **1** arrest cells in S phase without inducing DNA damage.

***2-R** Does Not Significantly Induce Apoptosis or Necrosis in BEL-7402 Cells.* As accumulated S phase arrest may induce apoptosis, we next examined whether **2-R** induces apoptosis by an Annexin V/PI double staining assay. Annexin V-positive cells slightly increased in the presence of **2-R** and **1**, and fewer than 20% cells were apoptotic in the presence of 100 nM **2-R** (Figure 7A,B).

Because **2-R** failed to significantly induce apoptosis, we further assessed whether **2-R** induces necrosis. A Trypan blue exclusion assay was performed after BEL-7402 cells were exposed to **2-R** or **1** for 72 h. As shown in Figure 7C, **2-R** slightly induced cell death in a dose-dependent manner, which is consistent with the results presented in Figure 7B, where **2-R** induced comparable late apoptosis in BEL-7402 cells.

***2-R** Exhibits Potent Activity against Multidrug-Resistant Cell Lines.* Multidrug resistance is one of the main causes of cancer treatment failure, and it often happens with drugs that originate from natural products. As **2-R** is modified from tylophorine, the activity of **2-R** against a number of well-characterized multidrug-resistant cell lines including K562-R, KB-R, and HL-60-R was studied (Table 4). As shown in Table 5, both **2-R** and **1** displayed similar antiproliferative activities against the resistant cell lines and their parental cell lines with resistant factor values of about 1, whereas the resistant cell lines were resistant to ADR, NVT, and VCR, respectively. These results indicated that multidrug-resistant cell lines are sensitive to **2-R**, demonstrating its potent ability to overcome multidrug

DOI: 10.1021/acs.jmedchem.6b01502
J. Med. Chem. XXXX, XXX, XXX−XXX

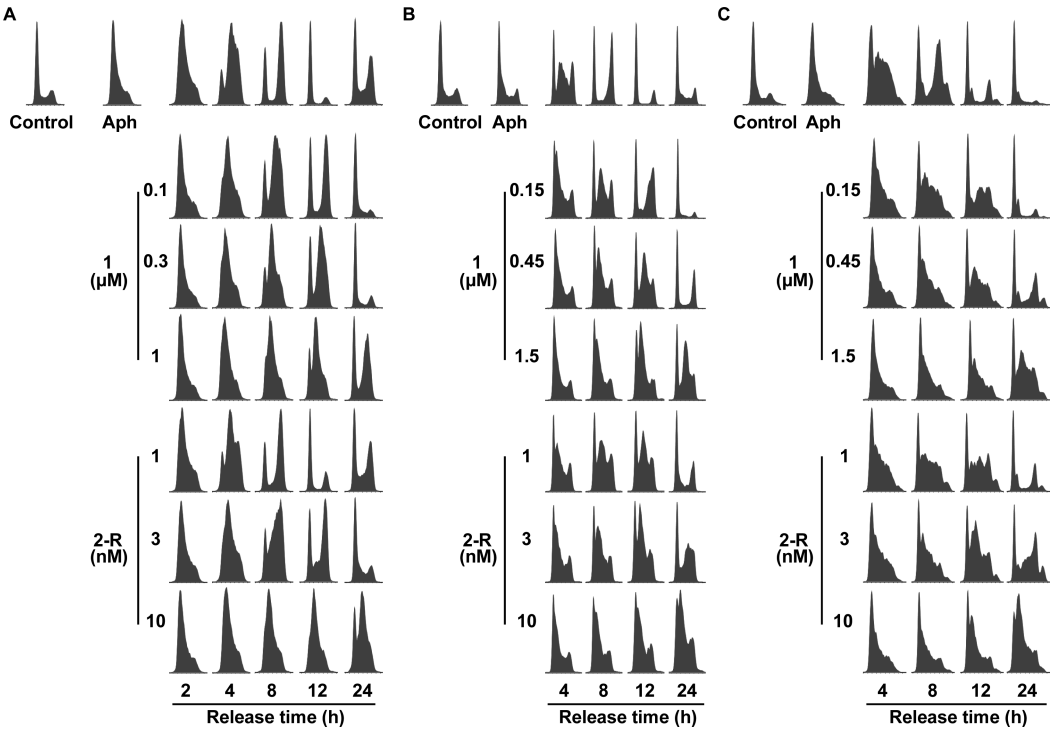

Figure 5. 2-R significantly delays S phase progression. BEL-7402 (A), SMMC-7721 (B), and ZIP-177 (C) cells were synchronized with aphidicolin in early S phase and then incubated with fresh media with or without test compounds for the indicated amount of time. Cell cycle distribution was determined with flow cytometry. Data shown are representative from three independent experiments.

resistance. To investigate whether this activity is due to a reduction in the expression of P-gp, we detected the protein level of P-gp in K562/ADR cells after treatment with compound **1** or **2-R** for 24 h. Compound **1** or **2-R** had little effect on the expression of P-gp (Figure S1), indicating that they did not overcome multidrug resistance by downregulating the expression of P-gp. The exact mechanism deserves further investigation.

To identify whether **2-R** affects S phase progression in multidrug-resistant cells, cells synchronized with aphdicolin, released, and incubated with the designated compounds for different lengths of time. As shown in Figure 8A,B, KB parental cells and multidrug-resistant cells entered G2-metaphase after 4 h in the absence of **1** or **2-R**, whereas both KB parental cells and multidrug-resistant cells remained in S phase up to 12 h upon treatment with **2-R** (10 nM), indicating that **2-R** delayed S phase progression in multidrug-resistant cells as well as in parental cells. This effect was confirmed in another pair of multidrug-resistant cells (K562/ADR) and its counterparts (Figure 8C,D).

DISCUSSION AND CONCLUSIONS

6-*O*-Desmethylcryptopleurine (**1**) as well as its ester and ether derivatives were synthesized and found to exert excellent antiproliferative activities against A549 and BEL-7402 cells, and compound **2-R** was found to possess the most potent activity in the primary screening. This study revealed that **2-R** significantly inhibits the proliferation of a panel of 30 cancer cell lines including 3 multidrug-resistant cell lines, with an average IC_{50} value of 2.1 nM, which is much lower than that of **1** (IC_{50}: 166.7 nM). **2-R** displayed a potent inhibitory effect against cell growth and colony formation. It induced cell cycle arrest in S phase, which was due to delayed S phase progression. Further study revealed that **2-R** significantly inhibited DNA synthesis without inducing DNA double-strand breaks. However, the molecular target for its inhibition of DNA synthesis needs to be clarified to better understand its mechanism of action. Furthermore, the anticancer activity of **2-R** is not due to the induction of apoptosis or cytotoxicity based on the following observations: first, **2-R** treatment up to 72 h failed to induce annexin V-positive cells or accumulate cells in sub-G1 phase; second, **2-R**-treated cells remained intact upon 72 h treatment; and third, **2-R** completely blocked cell proliferation up to 10 days without reducing cell number during the incubation. These results indicate that **2-R** may exert its selective cytostatic activity on rapidly proliferating cells while sparing non-proliferating cells. Though one important characteristic of tumor cells is uncontrolled proliferation, the safety of **2-R** should be carefully evaluated for further development. Finally, **2-R** displayed favorable activity against MDR cells with an RF value of about 1 and delayed S phase progression in MDR cell lines, which makes **2-R** an ideal drug candidate to overcome multiple drug resistance. These results together with further study on the safety profile and in vivo efficacy of **2-R** will facilitate the discovery of new phenanthroindolizidine and phenanthroquinolizidine alkaloids for use as anticancer drug candidates.

EXPERIMENTAL SECTION

Materials and Methods. *General.* ^{1}H and ^{13}C NMR spectra were obtained using a Bruker AV400 spectrometer in $CDCl_3$ or DMSO-d_6 with tetramethylsilane as the internal standard. HRMS data were obtained on an FTICR-MS instrument (Ionspec 7.0 T). The melting points were determined on an X-4 binocular microscope melting point apparatus and are uncorrected. Reaction progress was monitored by thin-layer chromatography on silica gel GF-254 with detection by UV. The enantiomeric excess of **2-rac**, **2-S**, and **2-R** was determined by

DOI: 10.1021/acs.jmedchem.6b01502
J. Med. Chem. XXXX, XXX, XXX−XXX

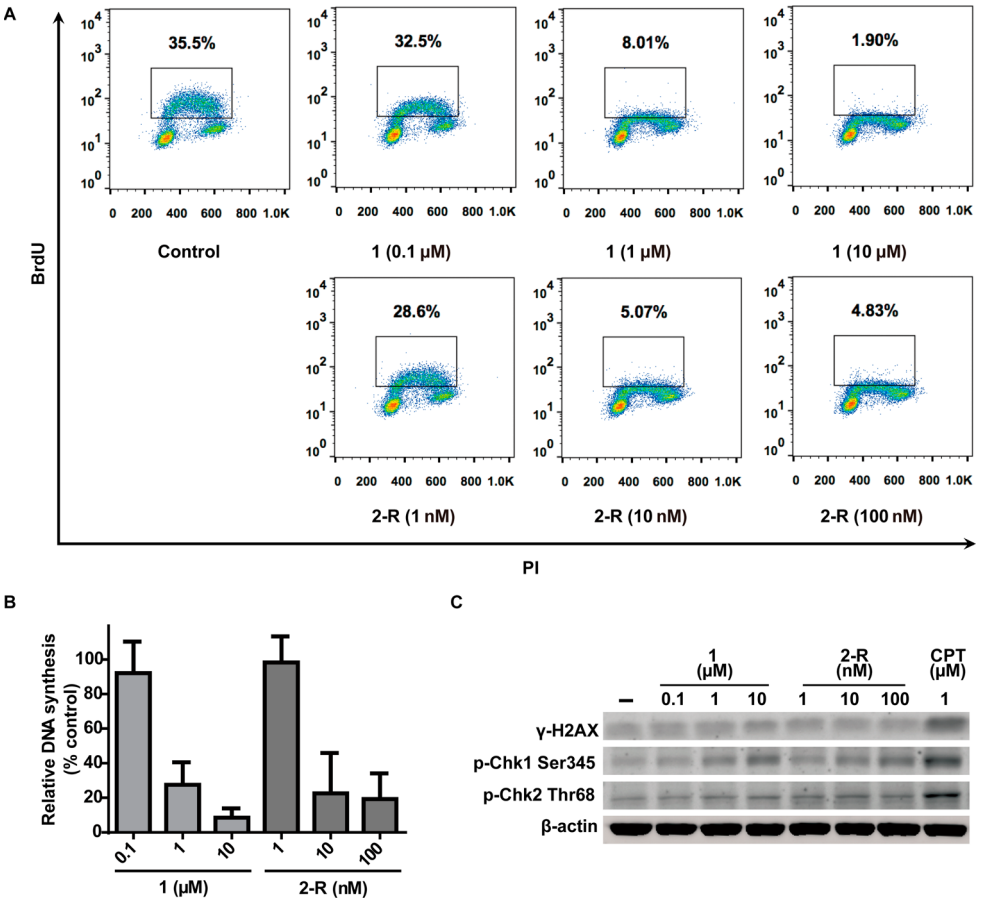

Figure 6. 2-R potently inhibits DNA synthesis without inducing DNA damage. BEL-7402 cells were treated with various concentrations of **2-R** or **1** for 1 h before cells were labeled with BrdU for 30 min. BrdU-positive cells were stained with an antibody and detected by flow cytometry. (A) Representative dot plots of BrdU incorporation. (B) Quantitation of relative DNA synthesis in the presence of **1** or **2-R**. Data shown are the mean + SD of three independent experiments. (C) Western blot of phospho-Chk1 Ser345, phospho-Chk2 Thr68, and γH2AX after treatment of BEL-7402 cells with the designated compounds for 1 h.

HPLC on a Shimadzu LC-20AT instrument with a ChiralPak AD-H column (250 mm, 4.6 mm, 5μ) using a mixture of hexane:isopropanol:triethyl amine (75:25:0.1) as the eluent at a flow rate of 1.0 mL/min under 254 nm. The purities of compounds **9**–**22** and **25** were all determined by HPLC on a Shimadzu LC-20AT instrument with a Silica column (250 mm, 4.6 mm, 5μ) using a mixture of dichloromethane:isopropanol (80:20) as the eluent and at a flow rate of 1.0 mL/min under 254 nm. All compounds used for biological tests were ≥95% pure.

Synthesis of (E)-2-(4-Acetoxyphenyl)-3-(3,4-dimethoxyphenyl)-acrylic Acid. A mixture of 3,4-dimethoxybenzaldehyde (19.6 g, 0.1 mol), 4-hydroxyphenylacetic acid (12.2 g, 0.1 mol), acetic anhydride (40 mL), and triethyl amine (20 mL) was refluxed under mechanical stirring. When the reaction was complete, water (60 mL) was added to the reaction mixture, and the reaction was refluxed for 1 h, cooled to room temperature with stirring for another 1 h, and then filtered. The cake was washed with water and ethanol and then dried to give (*E*)-2-(4-acetoxyphenyl)-3-(3,4-dimethoxyphenyl)acrylic acid (27.4 g, 87%) as a yellow solid. mp 243–246 °C; ^{1}H NMR (400 MHz, DMSO-d_6): δ 12.58 (br, 1H), 7.71 (s, 1H), 7.23 (d, *J* = 7.6 Hz, 2H), 7.16 (d, *J* = 7.6 Hz, 2H), 6.85–6.91 (m, 2H), 6.41 (s, 1H), 3.72 (s, 3H), 3.30 (s, 3H), 2.22 (s, 3H); ^{13}C NMR (400 MHz, DMSO-d_6): δ 169.1, 168.4, 149.9, 149.6, 147.8, 139.4, 134.3, 130.6, 129.7, 126.7, 125.3, 122.2, 111.8, 111.1, 55.3, 54.5, 20.8; HRMS (ESI): calcd. for $C_{19}H_{16}O_6$ $[M - H]^-$, 341.1031; found, 341.1031.

*Synthesis of (E)-Methyl 3-(3,4-Dimethoxyphenyl)-2-(4-hydroxyphenyl)acrylate (**3**).* A mixture of (*E*)-2-(4-acetoxyphenyl)-3-(3,4-dimethoxyphenyl)acrylic acid (10.0 g, 29.3 mmol), methanol (150 mL), and concentrated sulfuric acid (6.5 g) was refluxed for 4 h and then condensed to remove most of the methanol. When water (100 mL) was added, a large amount of solid precipitated. The solid was collected by filtration, washed with saturated sodium bicarbonate, and then dried to give **3** (9.0 g, 90%) as a white solid. mp 127–128 °C; ^{1}H NMR (400 MHz, $CDCl_3$): δ 7.77 (s, 1H), 7.11 (d, *J* = 8.4 Hz, 2H), 6.83–6.86 (m, 3H), 6.74 (d, *J* = 8.4 Hz, 1H), 6.49 (d, *J* = 1.6 Hz, 1H), 3.85 (s, 3H), 3.79 (s, 3H), 3.46 (s, 3H); ^{13}C NMR (400 MHz, $CDCl_3$): δ 169.3, 155.7, 149.9, 148.1, 140.7, 131.1, 129.6, 128.1, 127.4, 125.6, 115.9, 112.5, 110.5, 55.6, 55.1, 52.4. HRMS (ESI): calcd. for $C_{18}H_{18}NaO_5$ $[M + Na]^+$, 337.1046; found, 337.1041.

*Synthesis of Methyl 6-Hydroxy-2,3-dimethoxyphenanthrene-9-carboxylate (**4**).* To a solution of **3** (1.20 g, 3.82 mmol) in trifluoroacetic acid (20 mL) was added manganese dioxide (0.33 g, 3.82 mmol), and the mixture was stirred at room temperature for 6 h. When the reaction was complete, as indicated by TLC, acetic anhydride (20 mL) was added, and the mixture was then stirred at 40 °C for 4 h. Water was slowly added (50 mL) at room temperature, and the mixture was heated to 70 °C and monitored by TLC. When the reaction was complete, water and dichloromethane were added to the mixture; the water layer was separated and extracted with dichloromethane. The combined organic layer was washed with sodium bicarbonate, dried over sodium sulfate, filtered, and then concentrated. The residue was purified on silica gel column using petroleum ether and ethyl acetate (2:1) as eluent to give **4** (0.87 g, 73%) as a yellow solid. mp 188–190 °C; ^{1}H NMR (400 MHz, DMSO-d_6): δ 9.91 (s, 1H), 8.66 (d, *J* = 9.2 Hz, 1H), 8.26 (s, 1H), 8.03 (s, 1H), 7.94 (s, 1H), 7.59 (s, 1H), 7.18 (d, *J* = 8.8 Hz, 1H), 4.04 (s, 3H), 3.93 (s, 3H), 3.92 (s, 3H); ^{13}C NMR (400 MHz, $CDCl_3$): δ 168.2, 154.2, 150.9, 149.8, 131.9, 129.7, 128.5, 126.6, 125.6, 123.6, 123.2, 116.5, 109.2, 106.3,

DOI: 10.1021/acs.jmedchem.6b01502
J. Med. Chem. XXXX, XXX, XXX–XXX

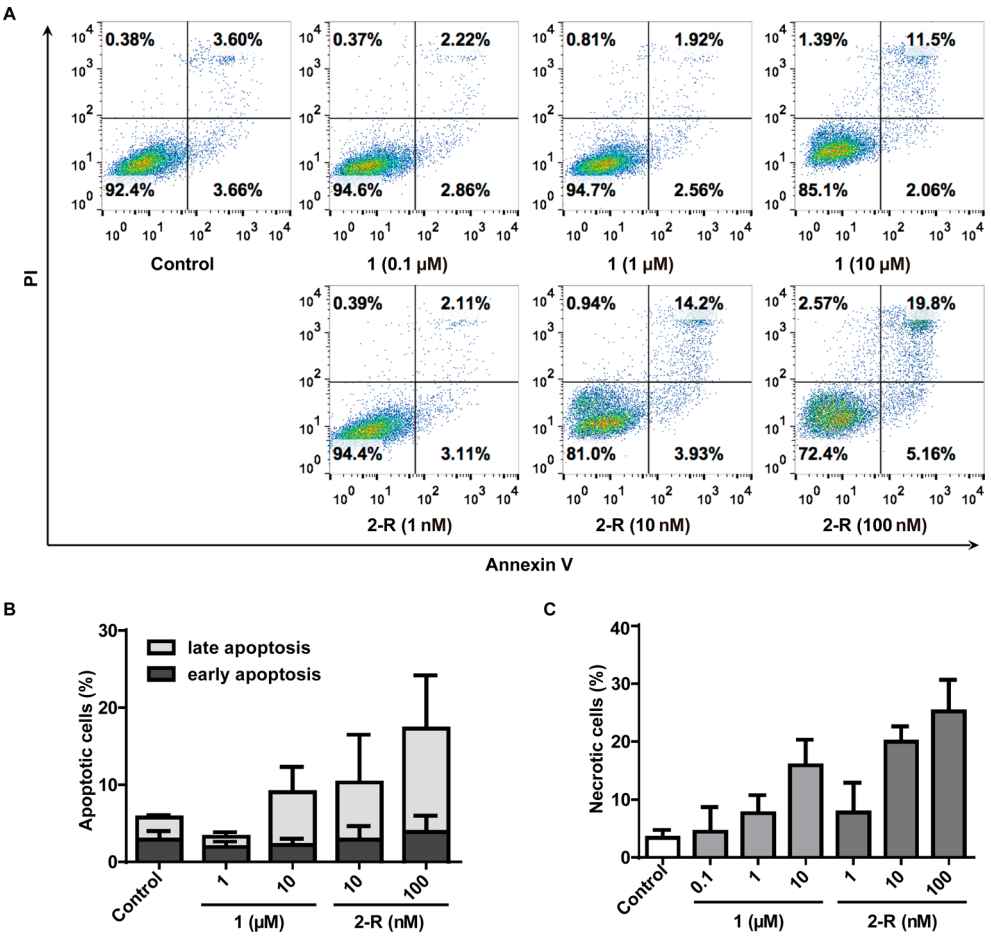

Figure 7. 2-R failed to induce a significant amount of cell apoptosis or necrosis. (A) BEL-7402 cells were treated with various concentrations of **2-R** or **1** for 72 h, and annexin V/PI labeling was performed. Representative dot plots obtained from flow cytometry are shown. (B) Quantitation of early and late apoptotic cells. (C) BEL-7402 cells were treated with various concentrations of **2-R** or **1** for 72 h, and necrotic cells were counted by a Trypan blue exclusion assay. Data shown are the mean + SD of three independent experiments.

Table 4. Background of Drug-Resistant Cell Lines

cell line	resistant drug	concentration (μM/L)	gene alteration
K562/ADR	ADR	2	P-gp overexpression
HL60/MX2	NVT	0.2	BCRP overexpression
KB/VCR	VCR	0.2	P-gp overexpression

103.2, 55.9, 52.2; HRMS (ESI): calcd. for $C_{18}H_{16}NaO_5$ $[M + Na]^+$, 335.0890; found, 335.0889.

*Synthesis of Methyl 6-(Benzyloxy)-2,3-dimethoxyphenanthrene-9-carboxylate (**5**).* A mixture of **4** (2.5 g, 8.02 mmol), anhydrous potassium carbonate (1.62 g, 12.02 mmol), benzyl bromide (1.65 g, 9.62 mmol), and dried acetone (50 mL) was refluxed for 8 h and then cooled to room temperature. To the mixture was added dichloromethane (100 mL), which was stirred and then filtered. The filtrate was condensed and then washed with petroleum ether and ethyl acetate (10:1) to give **5** (2.83 g, 88%) as a white solid. mp 156−157 °C; ^{1}H NMR (400 MHz, $CDCl_3$): δ 8.94 (d, J = 9.2 Hz, 1H), 8.32 (s, 1H), 7.98 (d, J = 2.8 Hz, 1H), 7.78 (s, 1H), 7.55 (d, J = 7.2 Hz, 2H), 740−7.45 (m, 2H), 7.34−7.38 (m, 2H), 7.26 (s, 1H), 5.31 (s, 2H),

Table 5. IC_{50} Values of 2-R and 1 against Parental and Drug-Resistant Cell Lines

	IC_{50} (mean ± SD, nM)				
cell line	**1**	**2-R**	ADR	NVT	VCR
K562/ADR	137.5 ± 29.4	2.6 ± 0.9	3310.2 ± 85.9		
K562	98.4 ± 16.8	2.2 ± 0.7	77.7 ± 2.5		
RF	1.4	1.2	42.6		
HL60/MX2	278.3 ± 33.7	1.7 ± 0.2		350.7 ± 87.9	
HL60	212.8 ± 100.1	1.8 ± 0.9		7.2 ± 4.4	
RF	1.3	0.9		48.7	
KB/VCR	65.2 ± 15.3	1 ± 0.2			238.7 ± 16
KB	58.2 ± 3.7	1.2 ± 0.2			0.2 ± 0.1
RF	1.1	0.8			1193.5
RF (mean)	1.26	0.96	42.6	48.7	1193.5

DOI: 10.1021/acs.jmedchem.6b01502
J. Med. Chem. XXXX, XXX, XXX−XXX

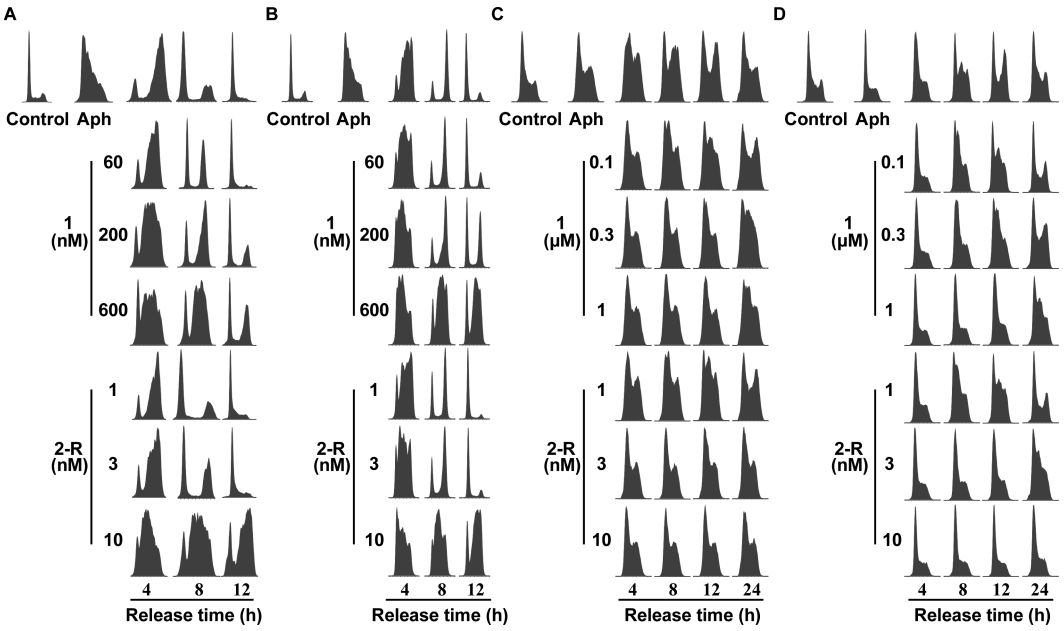

Figure 8. 2-R delays S phase progression in multidrug-resistant cells and their parental lines. KB (A), KB/VCR (B), K562 (C), and K562/ADR (D) cells were synchronized with aphidicolin in early S phase and then incubated with fresh media with or without the tested compounds for different amounts of time. Cell cycle distribution was determined with flow cytometry.

4.11 (s, 3H), 4.02 (s, 3H), 4.02 (s, 3H); ^{13}C NMR (400 MHz, $CDCl_3$): δ 168.2, 157.3, 150.9, 149.7, 136.9, 131.7, 129.6, 128.7, 128.5, 128.1, 127.6, 126.7, 125.6, 123.7, 123.3, 116.3, 109.2, 106.1, 103.1, 70.4, 56.1, 55.9, 52.1; HRMS (ESI): calcd. for $C_{25}H_{22}NaO_5$ $[M + Na]^+$, 425.1359; found, 425.1352.

*Synthesis of (6-(Benzyloxy)-2,3-dimethoxyphenanthren-9-yl)-methanol (**6**).* A suspension of ester **5** (2.19 g, 5.45 mmol) in dry tetrahydrofuran (250 mL) was added in small portions to a suspension of lithium aluminum hydride (0.62 g, 16.34 mmol) in dry tetrahydrofuran (150 mL) at ice-bath temperature. After the reaction mixture had been refluxed under dry nitrogen for 1 h, the mixture was cooled and acidified with diluted hydrochloric acid to pH 2. Water (100 mL) was added, and the precipitate was collected by filtration to afford **6** (1.94 g, 95%) as a white solid. mp 184−186 °C; ^{1}H NMR (400 MHz, $CDCl_3$): δ 8.10 (d, J = 8.8 Hz, 1H), 7.99 (d, J = 2.8 Hz, 1H), 7.78 (s, 1H), 7.53−7.56 (m, 3H), 7.40−7.45 (m, 2H), 7.30−7.38 (m, 2H), 7.19 (s, 1H), 5.29 (s, 2H), 5.14 (d, J = 6.0 Hz, 2H), 4.09 (s, 3H), 4.01 (s, 3H), 1.76 (t, J = 6.0 Hz, 1H); ^{13}C NMR (400 MHz, DMSO-d_6): δ 156.7, 149.4, 148.7, 137.3, 133.9, 131.0, 128.5, 127.9, 127.9, 126.7, 125.9, 123.8, 123.5, 121.9, 115.7, 108.6, 106.0, 104.0, 69.5, 61.6, 55.8, 55.4; HRMS (ESI): calcd. for $C_{24}H_{22}NaO_4$ $[M + Na]^+$, 397.1410; found, 397.1402.

*Synthesis of 6-(Benzyloxy)-10-bromo-9-(bromomethyl)-2,3-dimethoxyphenanthrene (**7**).* A solution of bromine (1.48 g, 9.25 mmol) in chloroform (20 mL) was added to a solution of alcohol **6** (3.19 g, 8.5 mmol) in chloroform (70 mL) at 0 °C. The mixture was stirred at room temperature for 10 h and was filtered and washed with petroleum ether and ethyl acetate (10:1) to afford **7** (3.75 g, 98%) as a white solid. mp 200−202 °C; ^{1}H NMR (400 MHz, $CDCl_3$): δ 7.99 (d, J = 8.8 Hz, 1H), 7.77 (s 1H), 7.66 (s, 1H), 7.58 (s, 1H), 7.52 (d, J = 7.2 Hz 2H), 7.43 (t, J = 7.2 Hz 2H), 7.37 (d, J = 7.2 Hz, 1H), 7.30 (d, J = 8.4 Hz, 1H), 5.23 (s, 2H), 5.14 (s, 2H), 4.03 (s, 6H); ^{13}C NMR (400 MHz, $CDCl_3$): δ 157.4, 149.92, 149.88, 136.8, 130.7, 129.3, 128.8, 128.2, 127.5, 126.4, 125.7, 125.3, 123.9, 122.8, 116.3, 109.2, 106.2, 103.0, 70.4, 56.0, 55.9, 32.8.

*Synthesis of 1-((6-(Benzyloxy)-10-bromo-2,3-dimethoxyphenanthren-9-yl)methyl)-N,N-diethylpiperidine-2-carboxamide (**8-rac**).* A solution of bromide **7** (3.0 g, 6.67 mmol), (DL)-*N,N*-diethylpyrrolidine-2-carboxamide (1.35 g, 7.33 mmol), and potassium carbonate (4.05 g, 29.3 mmol) in *N,N*-dimethylformamide (60 mL) was stirred for 1 h and heated at reflux for 8 h. After cooling, dichloromethane (60 mL) was added to the reaction mixture, and it was filtered. The filtrate was concentrated in vacuo, and the residue was purified on a silica gel column to give amide **8-rac** (3.75 g, 91%) as a white solid. mp 131−133 °C; ^{1}H NMR (400 MHz, $CDCl_3$): δ 9.07 (d, J = 8.8 Hz, 1H), 7.89 (s, 1H), 7.85 (s, 1H), 7.80 (s, 1H), 7.54−7.53 (m, 2H), 7.42−7.40 (m, 3H), 7.37−7.35 (m, 1H), 5.27 (s, 2H), 4.44 (d, J = 12.0 Hz, 1H), 4.17 (d, J = 12.0 Hz, 1H), 4.08 (s, 6H), 3.54−3.47 (m, 3H), 3.42−3.37 (m, 1H), 3.30 (d, J = 9.6 Hz, 1H), 2.91 (d, J = 10.4 Hz, 1H), 2.34−2.32 (m, 1H), 1.88−1.86 (m, 1H), 1.74 (s, 2H), 1.41−1.29 (m, 6H), 1.19−1.16 (m, 3H); ^{13}C NMR (400 MHz, $CDCl_3$): δ 172.6, 157.4, 149.6, 149.3, 137.2, 130.9, 130.5, 130.3, 128.7, 128.1, 127.6, 126.5, 125.9, 125.3, 123.1, 115.5, 109.7, 105.8, 103.3, 70.4, 57.8, 56.0, 50.5, 42.1, 40.9, 29.7, 25.3, 23.8, 15.0, 13.15. HRMS (ESI) calcd for $C_{34}H_{40}BrN_2O$ $[M + H]^+$, 619.2171, found, 619.2168.

*Synthesis of **8-S**.* Synthesis was performed according to the procedure for **8-rac** using (*S*)-*N,N*-diethylpyrrolidine-2-carboxamide instead of (DL)-N,N-diethylpyrrolidine-2-carboxamide. Yield, 90%.

*Synthesis of **8-R**.* Synthesis was performed according to the procedure for **8-rac** using (*R*)-*N,N*-diethylpyrrolidine-2-carboxamide instead of (DL)-N,N-diethylpyrrolidine-2-carboxamide. Yield, 91%.

*Synthesis of 6-Benzyloxy-2,3-dimethoxy-11,12,13,14,14a,15-hexahydro-15-hydroxy-9H-dibenzo[f,h]pyrido[1,2-b]isoquinoline (**9-rac**).* To a solution of amide **8-rac** (10.0 g, 16.18 mmol) and *N,N,N′,N′*-tetramethylethylenediamine (4.31 g, 37.21 mmol) in dry tetrahydrofuran (500 mL) at −78 °C was added a solution of *n*-BuLi in hexane (14.83 mL, 2.4 mol/L, 35.60 mmol), and the resulting mixture was stirred at this temperature for 5 h under Ar in the dark. Then, methanol (200 mL) and sodium borohydride (0.33 g, 70.65 mmol) were added to the mixture. After stirring at −40 °C for 1 h at room temperature for 8 h, the reaction mixture was quenched with water (200 mL) and the product was extracted with methylene dichloride (380 mL). The combined organic extracts were dried with anhydrous magnesium sulfate and concentrated in vacuo. The residue was purified by flash column chromatography on silica gel to give **9-rac** (6.0 g, 80%) as a white solid. Purity 97% (HPLC); dr 15:1 (NMR); mp 223−225 °C; ^{1}H NMR (400 MHz, $CDCl_3$): main component δ 8.18 (s, 1H), 8.04 (s, 1H), 7.65 (s, 1H), 7.63−7.57 (m, 3H), 7.44 (t, J = 7.3 Hz,2H), 7.38 (d, J = 7.2 Hz,1H), 7.28 (dd, J = 8.7, 1.5 Hz, 1H), 5.38 (s, 2H), 5.00 (d, J = 9.2 Hz,1H), 4.62 (d, J = 9.2 Hz,1H), 4.04 (s, 3H), 3.93 (s, 3H), 3.25 (d, J = 9.2 Hz, 1H), 2.97 (s, 1H), 2.1 (d, J = 12.0 Hz, 1H), 2.05 (d, J = 12.3 Hz, 1H), 1.83 (d, J = 10.6 Hz,1H), 1.75−1.65 (brs, 2H), 1.22−1.17 (m, 1H), 0.89−0.82 (m, 2H); ^{13}C

DOI: 10.1021/acs.jmedchem.6b01502
J. Med. Chem. XXXX, XXX, XXX−XXX

NMR (400 MHz, DMSO-d_6): δ 156.7, 149.1, 148.2, 137.2, 130.3, 128.5, 128.0, 127.9, 127.6, 126.0, 125.7, 124.4, 123.3, 122.4, 115.7, 105.9, 105.5, 104.2, 69.6, 65.6, 62.0, 55.8, 55.7, 55.4, 26.9, 25.0, 24.0; HRMS (ESI) calcd for $C_{30}H_{32}NO_4$ $[M + H]^+$, 470.2287; found, 470.2329.

*Synthesis of 9-(**14aS,15S**).* Synthesis was performed according to the procedure for **9-rac** using **8-S** instead of **8-rac**. Yield, 82%.

*Synthesis of 9-(**14aR,15R**).* Synthesis was performed according to the procedure for **9-rac** using **8-R** instead of **8-rac**. Yield, 81%.

*Synthesis of 2,3-Dimethoxy-11,12,13,14,14a,15-hexahydro-15-hydroxy-9H-dibenzo[f,h]pyrido[1,2-b]isoquinolin-6-ol (**10-rac**).* To a solution of **9-rac** (0.9 g, 1.92 mmol) in tetrahydrofuran (500 mL) and methanol (100 mL) was added Pd/C (10%, 0.09 g), and the resulting mixture was stirred at room temperature under a H_2 atomosphere for 2 days. After being diluted with dichloromethane (50 mL), the mixture was filtered. The filtrate was condensed to give **10-rac** (0.69 g, 95%) as a white solid. Purity 96% (HPLC); mp 234 °C (dec.); ^{1}H NMR (400 MHz, DMSO-d_6): δ 9.75 (s, 1H), 7.96 (s, 1H), 7.91 (s, 1H), 7.61 (s, 1H), 7.55 (d, J = 8.8 Hz, 1H), 7.03 (d, J = 8.8 Hz, 1H), 4.86 (d, J = 9.2 Hz, 1H), 4.58 (d, J = 9.2 Hz, 1H), 4.05 (d, J = 16.0 Hz, 1H), 4.01 (s, 3H), 3.92 (s, 3H), 3.24 (d, J = 16.0 Hz, 1H), 3.00 (d, J = 10.4 Hz, 1H), 2.84 (s, 1H), 2.13−1.98 (m, 3H), 1.82 (d, J = 11.6 Hz, 1H), 1.61−1.57 (m, 2H), 1.36−1.27 (m, 1H); ^{13}C NMR (400 MHz, DMSO-d_6): δ 156.4, 149.4, 148.5, 131.3, 127.3, 126.5, 126.4, 125.1, 123.5, 121.8, 116.8, 107.0, 106.0, 104.2, 67.5, 66.1, 62.7, 56.4, 56.3, 55.94, 27.5, 25.6, 24.6. HRMS (ESI) calcd for $C_{23}H_{26}NO_4$ $[M + H]^+$, 380.1862; found, 380.1862.

*Synthesis of 10-(**14aS,15S**).* Synthesis was performed according to the procedure for **10-rac** using **9-(14aS,15S)** instead of **9-rac**. Yield, 96%.

*Synthesis of 10-(**14aR,15R**).* Synthesis was performed according to the procedure for **10-rac** using **9-(14aR,15R)** instead of **9-rac**. Yield, 95%.

*Synthesis of 2,3-Dimethoxy-11,12,13,14,14a,15-hexahydro-9H-dibenzo[f,h]pyrido[1,2-b]isoquinolin-6-ol (**2-rac**).* To a solution of **10-rac** (0.69 g, 1.84 mmol) in trifluoroacetic acid (20 mL) was added triethylsilane (0.48 g, 4.21 mmol), and the resulting mixture was stirred at room temperature for 2 h in the dark. Dichloromethane (20 mL) was added, and the mixture was made basic with a 10% aqueous solution of sodium carbonate and then filtered. The filtrate was concentrated and washed with cold methanol to give **2-rac** (0.65 g, 96%) as a yellow solid. Purity 97% (HPLC); mp 175 °C (dec.); ^{1}H NMR (400 MHz, DMSO-d_6): δ 9.78 (s, 1H, OH), 7.98 (d, J = 1.8 Hz, 1H, 5-H), 7.92 (s, 1H, 4-H), 7.68 (d, J = 8.9 Hz, 1H, 8-H), 7.18 (s, 1H, 1-H), 7.11 (dd, J = 8.8, 1.9 Hz, 1H, 7-H), 4.38 (d, J = 15.6 Hz, 1H, 9-Ha), 4.00 (s, 3H, OCH_3), 3.91 (s, 3H, OCH_3), 3.51 (d, J = 14.5 Hz, 1H, 9-Hb), 3.22 (d, J = 9.9 Hz, 1H, 11-Ha), 3.00 (d, J = 14.7 Hz, 1H, 15-Ha), 2.70 (dd, J = 15.7, 10.9 Hz, 1H, 15-Hb), 2.43−2.15 (m, 2H, 11-Hb, 14a-H), 1.91 (d, J = 10.9 Hz, 1H, 13-Ha), 1.81−1.65 (m, 2H, 12-Hb, 14-Ha), 1.60 (d, J = 12.1 Hz, 1H, 12-Ha), 1.46−1.27 (m, 2H, 13-Hb, 14-Hb); ^{13}C NMR (400 MHz, DMSO-d_6): δ 155.5 (C-6), 149.1 (C-2 or C-3), 148.2 (C-3 or C-2), 130.0, 125.4, 125.2, 123.9 (C-8), 123.0, 122.7, 121.6, 116.3 (C-7), 106.6 (C-5), 104.0 (C-1 or C-4), 103.9 (C-4 or C-1), 57.2 (C-14a), 55.5 (OCH_3), 55.4 (OCH_3), 55.2 (C-11), 54.9 (C-9), 33.3 (C-15), 32.6 (C-13), 25.0 (C-12), 23.5 (C-14); HRMS (ESI) calcd for $C_{23}H_{26}NO_3$ $[M + H]^+$, 364.1913; found, 364.1916.

*Synthesis of **2-S**.* Synthesis was performed according to the procedure for **2-rac** using **10-(14aS,15S)** instead of **10-rac**. Yield, 94%. $[\alpha]_D^{20}$ = 114°, (c = 1.0, DMSO); purity 98% (HPLC); 98% ee [t_R (minor) = 12.43 min, t_R (major) = 18.68 min].

*Synthesis of **2-R**.* Synthesis was performed according to the procedure for **2-rac** using **10-(14aR,15R)** instead of **10-rac**. Yield, 94%. $[\alpha]_D^{20}$ = −112°, (c = 1.0, DMSO); purity 98% (HPLC); 99% ee [t_R (major) = 12.36 min, t_R (minor) = 18.68 min].

*Synthesis of 2,3-Dimethoxy-11,12,13,14,14a,15-hexahydro-9H-dibenzo[f,h]pyrido[1,2-b]isoquinolin-6-yl Acetate (**11**).* To a solution of **2-rac** (0.4 g, 1.1 mmol) in dichloromethane (50 mL) were added acetic anhydride (0.22 g, 2.2 mmol) and triethyl amine (0.17 g, 1.65 mmol), and then the mixture was stirred at room temperature for 3 h. After adding saturated sodium bicarbanate, the two phases were separated. The water layer was extracted with dichloromethane three times. The combined organic layer was washed with brine, dried with anhydrous magnesium sulfate, filtered, and concentrated in vacuo. The residue was purified by flash column chromatography on silica gel (dichloromethane:methanol 40:1 as eluent) to give **11** as a light-yellow solid (0.3 g, 67%). mp 176 °C; purity 95% (HPLC); ^{1}H NMR (400 MHz, $CDCl_3$): δ 8.13 (s, 1H), 7.78 (s, 2H), 7.27 (s, 1H), 7.14 (s, 1H), 4.43 (d, J = 15.4 Hz, 1H), 4.07 (s, 3H), 4.02 (s, 3H), 3.55 (d, J = 15.4 Hz, 1H), 3.29 (d, J = 9.9 Hz, 1H), 2.98−2.82 (m, 2H), 2.39 (s, 3H), 2.32−2.27 (m, 2H), 1.97 (d, J = 9.9 Hz, 1H), 1.88−1.78 (m, 3H), 1.59−1.50 (m, 1H), 1.41 (s, 1H); ^{13}C NMR (400 MHz, $CDCl_3$): δ 169.9, 149.5, 148.5, 148.4, 129.7, 126.7, 126.5, 126.1, 124.8, 123.9, 123.5, 120.0, 114.4, 103.7, 57.3, 56.0, 55.9, 55.5, 34.2, 33.2, 25.5, 24.1, 22.1, 21.3; HRMS (ESI) calcd for $C_{25}H_{28}NO_4$ $[M + H]^+$, 406.2018; found, 406.2010.

*Synthesis of 2,3-Dimethoxy-11,12,13,14,14a,15-hexahydro-9H-dibenzo[f,h]pyrido [1,2-b]isoquinolin-6-yl Pivalate (**12**).* To a solution of **2-rac** (0.5 g, 1.38 mmol) in dichloromethane (50 mL) were succesively added triethyl amine (0.28 g, 2.75 mmol), DMAP (0.025 g, 0.21 mmol), and pivaloyl chloride. The mixture was stirred at room temperature for 4 h and was then quenched with suturated ammonium chloride. The organic layler was separated, and the water layer was extracted with dichloromethane three times. The combined organic layer was washed with brine, dried with anhydrous magnesium sulfate, filtered, and concentrated in vacuo. The residue was purified by flash column chromatography on silica gel (dichloromethane:methanol 40:1 as eluent) to give **12** as a light-yellow solid (0.47 g, 77%). mp 92−94 °C; purity 95% (HPLC); ^{1}H NMR (400 MHz, $CDCl_3$): δ 8.14 (d, J = 2.1 Hz, 1H), 7.87−7.85 (m, 2H), 7.27−7.23 (m, 2H), 4.46 (d, J = 15.5 Hz, 1H), 4.12 (s, 3H), 4.07 (s, 3H), 3.67 (d, J = 15.5 Hz, 1H), 3.30 (d, J = 11.2 Hz, 1H), 3.13 (dd, J = 3.1 Hz, J = 16.5 Hz, 1H), 2.96−2.89 (m, 1H), 2.46−2.41 (m, 1H), 2.33 (td, J = 3.6 Hz, J = 11.2 Hz, 1H), 2.06 (dd, J = 2.0 Hz, J = 11.2 Hz, 1H), 1.89 (d, J = 11.8 Hz, 1H), 1.81−1.77 (m, 2H), 1.61−1.50 (m, 2H), 1.45 (s, 9H); ^{13}C NMR (400 MHz, $CDCl_3$): δ 177.5, 149.6, 148.9, 148.6, 129.8, 126.7, 126.5, 126.2, 125.1, 123.9, 123.6, 120.0, 114.3, 103.9, 103.8, 57.4, 56.1, 55.9, 55.8, 39.2, 34.5, 33.4, 27.3 (3C), 27.2, 25.7, 24.2; HRMS (ESI) calcd for $C_{28}H_{34}NO_4$ $[M + H]^+$, 448.2488; found, 406.2483.

*Synthesis of 2,3-Dimethoxy-11,12,13,14,14a,15-hexahydro-9H-dibenzo[f,h]pyrido[1,2-b]isoquinolin-6-yl Cyclopropanecarboxylate (**13**).* To a solution of **2-rac** (0.4 g, 1.1 mmol) in dichloromethane (50 mL) were succesively added cyclopropanecarboxylic acid (0.12 g, 1.38 mmol), 1-ethyl-3-(3-(dimethylamino)propyl)carbodiimide hydrochloride (0.43 g, 2.2 mmol), triethyl amine (0.22 g, 2.2 mmol), and DMAP (0.27 g, 2.2 mmol). The mixture was stirred at room temperature overnight in the dark and was then quenched with suturated ammonium chloride. The organic layler was separated, and the water layer was extracted with dichloromethane three times. The combined organic layer was washed with brine, dried with anhydrous magnesium sulfate, filtered, and concentrated in vacuo. The residue was purified by flash column chromatography on silica gel (dichloromethane:methanol 80:1 as eluent) to give **13** (0.35 g, 8.03 mmol, yield 73%) as a light-yellow solid. mp 224−226 °C; purity 99% (HPLC); ^{1}H NMR (400 MHz, $CDCl_3$): δ 8.18 (d, J = 2.2 Hz, 1H), 7.86−7.84 (m, 2H), 7.29 (dd, J = 8.8 Hz, J = 2.2 Hz, 1H), 7.24 (s, 1H), 4.45 (d, J = 15.5 Hz, 1H), 4.10 (s, 3H), 4.06 (s, 3H), 3.65 (d, J = 15.0 Hz, 1H), 3.29 (d, J = 11.0 Hz, 1H), 3.10 (dd, J = 16.4 Hz, J = 3.2 Hz, 1H), 2.94−2.87 (m, 1H), 2.43−2.38 (m, 1H), 2.35−2.29 (m, 1H), 2.05 (d, J = 12.4 Hz, 1H), 1.98−1.93 (m, 1H), 1.92−1.88 (m, 1H), 1.81−1.77 (m, 1H), 1.57−1.46 (m, 2H), 1.27−1.24 (m, 2H), 1.11−1.06 (m, 2H); ^{13}C NMR (400 MHz, $CDCl_3$): δ 173.9, 149.6, 148.6, 148.6, 129.8, 126.8, 126.6, 126.3, 125.3, 123.9, 123.6, 120.1, 114.4, 103.9, 103.8, 57.5, 56.2, 56.0, 56.0 (2C), 34.7, 33.6, 25.8, 24.3, 13.2, 9.4 (2C); HRMS (ESI) calcd for $C_{27}H_{30}NO_4$ $[M + H]^+$, 432.2175; found, 432.2169.

*Synthesis of 2,3-Dimethoxy-11,12,13,14,14a,15-hexahydro-9H-dibenzo[f,h]pyrido[1,2-b]isoquinolin-6-yl Cyclohexanecarboxylate (**14**).* Synthesis was performed according to the procedure for **13** using cyclohexanecarboxylic acid. Obtained 0.41 g (yield 79%) as a

DOI: 10.1021/acs.jmedchem.6b01502
J. Med. Chem. XXXX, XXX, XXX−XXX

light yellow solid. mp 199−200 °C; purity 98% (HPLC); ^{1}H NMR (400 MHz, $CDCl_3$): δ 8.14 (s, 1H), 7.84−7.82 (m, 2H), 7.26−7.25 (m, 1H), 7.24 (s, 1H), 4.49 (d, J = 15.7 Hz, 1H), 4.10 (s, 3H), 4.06 (s, 3H), 3.71 (d, J = 14.6 Hz, 1H), 3.33 (d, J = 11.2 Hz, 1H), 3.13 (d, J = 16.0 Hz, 1H), 3.00−2.94 (m, 1H), 2.70−2.62 (m, 1H), 2.49 (s, 1H), 2.40−2.34 (m, 1H), 2.18 (s, 1H), 2.15 (s, 1H), 1.92−1.86 (m, 6H), 1.75−1.60 (m, 4H), 1.52−1.31 (m, 4H); ^{13}C NMR (400 MHz, $CDCl_3$): δ 174.9, 149.6, 148.7, 148.6, 129.8, 126.6, 126.4, 126.1, 123.8, 123.6, 120.1, 114.3, 103.8, 103.7, 57.5, 56.0, 55.9, 55.8, 43.4, 34.3, 33.3, 29.08, 29.06, 25.8, 25.6, 25.5, 24.0; HRMS (ESI) calcd for $C_{30}H_{36}NO_4$ $[M + H]^+$, 474.2644; found, 474.2625.

*Synthesis of 2,3-Dimethoxy-11,12,13,14,14a,15-hexahydro-9H-dibenzo[f,h]pyrido[1,2-b]isoquinolin-6-yl Furan-2-carboxylate (**15**).* Synthesis was performed according to the procedure for **13** using 2-furoic acid. Yield, 82%. mp 239−242 °C; purity 97% (HPLC); ^{1}H NMR (400 MHz, $CDCl_3$): δ 8.28 (s, 1H), 7.84 (d, J = 8.7 Hz, 1H), 7.79 (s, 1H), 7.69 (s, 1H), 7.45 (s, 1H), 7.38 (d, J = 8.3 Hz, 1H), 7.17 (s, 1H), 6.61 (s, 1H), 4.38 (d, J = 15.2 Hz, 1H), 4.06 (s, 3H), 4.04 (s, 3H), 3.55 (d, J = 15.2 Hz, 1H), 3.24 (d, J = 12.0 Hz, 1H), 2.99 (d, J = 15.7 Hz, 1H), 2.85−2.79 (m, 1H), 2.28−2.23 (m, 1H), 1.99 (d, J = 10.6 Hz, 1H), 1.87 (d, J = 11.0 Hz, 1H), 1.79 (s, 2H), 1.54−1.40 (m, 2H); ^{13}C NMR (400 MHz, $CDCl_3$): δ 156.3, 148.4, 147.4, 146.8, 146.2, 143.1, 128.7, 125.9, 125.8, 125.2, 124.3, 123.0, 122.4, 118.7, 118.5, 113.5, 111.2, 102.7, 102.6, 56.3, 55.2, 55.0, 54.9, 54.0, 33.8, 32.7, 24.9, 23.3; HRMS (ESI) calcd for $C_{28}H_{28}NO_5$ $[M + H]^+$, 458.1967; found, 458.1963.

*Synthesis of 2,3-Dimethoxy-11,12,13,14,14a,15-hexahydro-9H-dibenzo[f,h]pyrido[1,2-b]isoquinolin-6-yl Thiophene-2-carboxylate (**16**).* Synthesis was performed according to the procedure for **13** using thiophene-2-carboxylic acid. Obtained 0.45 g (yield 87%) as a light yellow solid. mp 247−249 °C; purity 98% (HPLC); ^{1}H NMR (400 MHz, $CDCl_3$): δ 8.28 (s, 1H), 8.04 (s, 1H), 7.86−7.81 (m, 2H), 7.69 (s, 1H), 7.39 (d, J = 8.0 Hz, 1H), 7.19 (s, 2H), 4.41 (d, J = 15.2 Hz, 1H), 4.07 (s, 3H), 4.05 (s, 3H), 3.58 (d, J = 15.1 Hz, 1H), 3.25 (d, J = 15.1 Hz, 1H), 3.03 (d, J = 15.8 Hz, 1H), 2.88−2.81 (s, 1H), 2.32−2.25 (s, 2H), 2.01 (d, J = 9.8 Hz, 1H), 1.87 (d, J = 11.8 Hz, 1H), 1.80 (s, 2H), 1.56−1.41 (m, 2H); ^{13}C NMR (400 MHz, $CDCl_3$): δ 161.0, 149.6, 148.6, 148.3, 134.8, 133.6, 133.0, 129.8, 128.1, 127.0, 126.9, 126.3, 125.5, 124.0, 123.6, 120.0, 114.6, 103.9, 103.8, 57.5, 56.3, 56.1, 56.02, 55.97, 34.9, 33.8, 25.9, 24.8, 24.3; HRMS (ESI) calcd for $C_{28}H_{28}NO_4S$ $[M + H]^+$, 474.1739; found, 474.1732.

*Synthesis of 2,3-Dimethoxy-11,12,13,14,14a,15-hexahydro-9H-dibenzo[f,h]pyrido[1,2-b]isoquinolin-6-yl Nicotinate (**17**).* Synthesis was performed according to the procedure for **13** using nicotinic acid. Obtained 0.51 g (yield 80%) as a light yellow solid. mp 183 °C (dec.); purity 96% (HPLC); ^{1}H NMR (400 MHz, $CDCl_3$): δ ^{1}H NMR (400 MHz, $CDCl_3$): δ 9.49 (s, 1H), 8.89 (dd, J = 4.8 Hz, J = 1.4 Hz, 1H), 8.55−8.52 (m, 1H), 8.32 (d, J = 2.0 Hz, 1H), 7.92 (d, J = 9.0 Hz, 1H), 7.86 (s, 1H), 7.52−7.49 (m, 1H), 7.41 (dd, J = 8.0 Hz, J = 2.0 Hz, 1H), 4.48 (d, J = 15.4 Hz, 1H), 4.09 (s, 3H), 4.07 (s, 3H), 3.68 (d, J = 15.4 Hz, 1H), 3.31 (d, J = 11.1 Hz, 1H), 3.14 (dd, J = 16.8 Hz, J = 3.2 Hz, 1H), 3.10−2.90 (m, 1H), 2.44 (t, J = 10.6 Hz, 1H), 2.34 (td, J = 10.8 Hz, J = 3.9 Hz, 1H), 2.10−2.06 (m, 1H), 1.91 (d, J = 12.8 Hz, 1H), 1.84−1.79 (m, 2H), 1.62−1.53 (m, 1H), 1.51−1.42 (m, 1H); ^{13}C NMR (400 MHz, $CDCl_3$): δ 164.3, 154.1, 151.5, 149.7, 148.7, 148.3, 137.7, 129.9, 127.0, 126.9, 126.3, 125.7, 125.0, 124.1, 123.5, 119.8, 114.5, 106.5, 103.8, 103.8, 57.5, 56.1, 56.0, 56.0, 55.9, 34.6, 33.5, 25.7, 24.2; HRMS (ESI) calcd for $C_{29}H_{29}N_2O_4$ $[M + H]^+$, 469.2127; found, 469.2120.

*Synthesis of 2,3-Dimethoxy-11,12,13,14,14a,15-hexahydro-9H-dibenzo[f,h]pyrido[1,2-b]isoquinolin-6-yl Benzo[d][1,2,3]-thiadiazole-7-carboxylate (**18**).* Synthesis was performed according to the procedure for **13** using benzo[d][1,2,3]thiadiazole-7-carboxylic acid. Obtained 0.48 g (yield 83%) as a yellow-green solid. mp 159−161 °C; purity 98% (HPLC); ^{1}H NMR (400 MHz, $CDCl_3$): δ 8.77 (d, J = 8.0 Hz, 1H), 8.49 (d, J = 8.0 Hz, 1H), 8.29 (s, 1H), 7.80 (d, J = 9.2 Hz, 1H), 7.67 (s, 2H), 7.36 (d, J = 8.8 Hz, 1H), 7.11 (s, 1H), 4.31 (d, J = 15.6 Hz, 1H), 4.05 (s, 3H), 4.01 (s, 3H), 3.48 (d, J = 15.6 Hz, 1H), 3.24 (d, J = 10.8 Hz, 1H), 2.96 (d, J = 16.0 Hz, 1H), 2.83−2.75 (m, 1H), 2.29−2.23 (m, 2H), 2.01 (d, J = 11.6 Hz, 1H), 1.90 (d, J = 11.6 Hz, 1H), 1.80−1.75 (m, 2H), 1.55−1.42 (m, 2H); ^{13}C NMR (400 MHz, $CDCl_3$): δ 164.2, 158.7, 149.4, 148.3, 148.0, 140.7, 131.1, 129.7, 129.1, 127.2, 127.1, 126.9, 126.1, 125.2, 124.1, 123.3, 122.3, 119.2, 114.6, 103.7, 103.5, 57.3, 56.3, 55.9, 53.5, 34.9, 33.8, 26.0, 24.4; HRMS (ESI) calcd for $C_{30}H_{28}N_3O_4S$ $[M + H]^+$, 526.1801; found, 526.1788.

*Synthesis of 2-((2,3-Dimethoxy-11,12,13,14,14a,15-hexahydro-9H-dibenzo[f,h]pyrido[1,2-b]isoquinolin-6-yl)oxy)acetamide (**19**).* To a solution of **2-rac** (0.5 g, 1.38 mmol) in DMF (9 mL) was added cesium carbonate (0.54 g, 1.66 mmol). After stirring at room temperature for 0.5 h, a solution of ethyl α-bromoacetamide (0.23 g, 1.65 mmol) in DMF (6 mL) was added dropwise under an ice bath. The reaction mixture was then stirred at room temperature and monitored by TLC. After the reaction was complete, ethyl acetate and water were added. The organic layler was separated, and the water layer was extracted with ethyl acetate three times. The combined organic layer was washed with brine, dried with anhydrous magnesium sulfate, filtered, and concentrated in vacuo. The residue was purified by flash column chromatography on silica gel (ethyl acetate as eluent) to give **19** as a brown solid (0.40 g, 69%). mp 205−207 °C; purity 96% (HPLC); ^{1}H NMR (400 MHz, DMSO-d_6): δ 8.11 (s, 1H), 8.04 (s, 1H), 7.80 (d, J = 8.8 Hz, 1H), 7.69 (s, 1H), 7.53 (s, 1H), 7.28−7.24 (m, 2H), 4.68 (s, 2H), 4.31 (d, J = 16.0 Hz, 1H), 4.02 (s, 3H), 3.93 (s, 3H), 3.40 (d, J = 16.0 Hz, 1H), 3.19−3.05 (m, 2H), 2.73−2.66 (m, 1H), 2.21−2.10 (m, 2H), 1.93 (d, J = 9.2 Hz, 1H), 1.78 (d, J = 8.8 Hz, 1H), 1.71 (d, J = 11.6 Hz, 1H), 1.63−1.54 (m, 1H), 1.39−1.32 (m, 2H); ^{13}C NMR (400 MHz, DMSO-d_6): δ 170.2, 155.6, 149.3, 148.2, 129.5, 125.7, 125.3, 124.7, 124.1, 123.2, 122.8, 115.8, 105.9, 104.4, 103.9, 67.1, 57.3, 55.7, 55.5, 55.4, 55.3, 33.9, 33.1, 25.5, 24.0; HRMS (ESI) calcd for $C_{25}H_{29}N_2O_4$ $[M + H]^+$, 421.2083; found, 421.2127.

*Synthesis of 2,3-Dimethoxy-6-(prop-2-yn-1-yloxy)-11,12,13,14,14a,15-hexahydro-9H-dibenzo[f,h]pyrido[1,2-b]-isoquinoline. (**20**).* Synthesis was performed according to the procedure for **19** using propargyl bromide instead of α-bromoacetamide. Obtained 0.47 g (yield 85%) as a brown solid. mp 202−204 °C; purity 96% (HPLC); ^{1}H NMR (400 MHz, $CDCl_3$): δ 8.03 (d, J = 2.5 Hz, 1H), 7.90 (s, 1H), 7.80 (d, J = 9.0 Hz, 1H), 7.26−7.22 (m, 2H), 4.89 (s, 2H), 4.42 (d, J = 15.5 Hz, 1H), 4.10 (s, 3H), 4.06 (s, 3H), 3.62 (d, J = 15.4 Hz, 1H), 3.26 (d, J = 11.3 Hz, 1H), 3.09 (dd, J = 16.3, J = 3.1 Hz, 1H), 2.90−2.86 (m, 1H), 2.60 (s, 1H), 2.40−2.34 (m, 1H), 2.29 (td, J = 11.2, J = 3.9 Hz, 1H), 2.03 (d, J = 13.1 Hz, 1H), 1.89 (d, J = 12.4 Hz, 1H), 1.79−1.72 (m, 2H), 1.57−1.42 (m, 2H); ^{13}C NMR (400 MHz, DMSO-d_6): δ 155.2, 149.3, 148.3, 129.6, 125.8, 125.4, 124.8, 124.1, 123.3, 122.8, 115.6, 106.5, 104.6, 104.0, 79.4, 78.2, 57.2, 55.9, 55.5, 55.4, 35.8, 34.0, 33.2, 30.7, 25.5, 24.0; HRMS (ESI) calcd for $C_{26}H_{28}NO_3$ $[M + H]^+$, 402.2024; found, 402.2604.

*Synthesis of 2-((2,3-Dimethoxy-11,12,13,14,14a,15-hexahydro-9H-dibenzo[f,h]pyrido[1,2-b]isoquinolin-6-yl)oxy)acetonitrile (**21-rac**).* Synthesis was performed according to the procedure for **19** using α-bromoacetonitrile instead of α-bromoacetamide. Obtained 0.45 g (yield 87%) as a brown solid. mp 199−201 °C; purity 95% (HPLC); ^{1}H NMR (400 MHz, $CDCl_3$): δ 7.94 (s, 1H), 7.79−7.75 (m, 2H), 7.20−7.16 (m, 2H), 4.92 (s, 2H), 4.39 (d, J = 16.0 Hz, 1H), 4.08 (s, 3H), 4.04 (s, 3H), 3.57 (d, J = 16.0 Hz, 1H), 3.27 (d, J = 8.0 Hz, 1H), 3.00 (d, J = 16.0 Hz, 1H), 2.87−2.81 (m, 1H), 2.35−2.26 (m, 2H), 2.04−1.99 (m, 1H), 1.88 (d, J = 16.0 Hz, 1H), 1.80−1.75 (m, 2H), 1.58−1.52 (m, 1H), 1.44−1.41 (m, 1H); ^{13}C NMR (400 MHz, DMSO-d_6): δ 162.3, 154.2, 149.4, 148.4, 129.5, 125.8, 125.3, 124.4, 123.9, 122.8, 116.8, 115.3, 106.7, 104.7, 103.9, 57.0, 55.9, 55.4, 53.9, 35.7, 33.8, 33.0, 30.7, 25.4, 23.9; HRMS (ESI) calcd for $C_{25}H_{27}N_2O_3$ $[M + H]^+$, 403.1977; found, 403.2016.

*Synthesis of **21-(S)**.* Synthesis was performed according to the procedure for **21-rac** using **2-S** instead of **2-rac**. Purity 95% (HPLC).

*Synthesis of **21-(R)**.* Synthesis was performed according to the procedure for **21-rac** using **2-R** instead of **2-rac**. Purity 95% (HPLC).

*Syntheisis of Ethyl 2-((2,3-Dimethoxy-11,12,13,14,14a,15-hexahydro-9H-dibenzo[f,h]pyrido[1,2-b]isoquinolin-6-yl)oxy)acetate (**22**).* Synthesis was performed according to the procedure for **19** using ethyl α-bromoacetate instead of α-bromoacetamide. Obtained 0.50 g (yield 81%) as a brown solid. mp 84−86 °C; purity 96% (HPLC); ^{1}H NMR (400 MHz, $CDCl_3$): δ 7.96 (d, J = 2.5 Hz, 1H), 7.87 (s, 1H),

DOI: 10.1021/acs.jmedchem.6b01502
J. Med. Chem. XXXX, XXX, XXX−XXX

7.77 (d, J = 9.0 Hz, 1H), 7.23 (s, 1H), 7.19 (dd, J = 9.0, J = 2.5 Hz, 1H), 4.81 (s, 2H), 4.53 (d, J = 15.4 Hz, 1H), 4.32 (q, J = 7.1 Hz, 2H), 4.10 (s, 3H), 4.06 (s, 3H), 3.61 (d, J = 15.4 Hz, 1H), 3.27 (d, J = 10.8 Hz, 1H), 3.06 (d, J = 8.4 Hz, 1H), 2.89 (t, J = 10.8 Hz, 1H), 2.38 (s, 1H), 2.30 (t, J = 10.4 Hz, 1H), 2.06 (d, J = 12.8 Hz, 1H), 1.92 (s, 1H), 1.84 (s, 2H), 1.66 (d, J = 12.4 Hz, 1H), 1.48 (s, 1H), 1.32 (t, J = 7.1 Hz, 3H); ^{13}C NMR (400 MHz, $CDCl_3$): δ 169.1, 155.6, 149.5, 148.4, 130.1, 126.5, 125.4, 125.1, 124.3, 124.3, 123.4, 114.5, 106.7, 103.8, 103.8, 65.9, 61.5, 57.5, 56.2, 56.0, 56.0, 34.7, 33.7, 25.9, 24.3, 14.3; HRMS (ESI) calcd for $C_{27}H_{32}NO_5$ $[M + H]^+$, 450.2236; found, 450.2275.

*Synthesis of 2-((2,3-Dimethoxy-11,12,13,14,14a,15-hexahydro-9H-dibenzo[f,h]pyrido[1,2-b]isoquinolin-6-yl)oxy)ethanol (**23**).* Under an ice bath, $LiAlH_4$ (0.06 g, 1.34 mmol) was added to a solution of **22** (0.3 g, 0.67 mmol) in tetrahydrofuran (20 mL) in portions. After the mixture was stirred at room temperature for 8 h, water was slowly added to quench the reaction, and the mixture was extracted with dichloromethane three times. The combined organic layer was washed with brine, dried with anhydrous magnesium sulfate, filtered, and concentrated in vacuo. The residue was purified by flash column chromatography on silica gel (dichloromethane:methanol 30:1 as eluent) to give **23** as a yellow-green solid (0.23 g, 84%). mp 223−225 °C; ^{1}H NMR (400 MHz, DMSO-d_6): δ 8.07−8.04 (m, 2H), 7.74 (d, J = 9.2 Hz, 1H), 7.22−7.18 (m, 2H), 4.98 (s, 1H), 4.30−4.22 (m, 3H), 4.01 (s, 3H), 3.91 (s, 3H), 3.84−3.82 (m, 2H), 3.37 (d, J = 16.0 Hz, 1H), 3.12 (d, J = 10.8 Hz, 1H), 2.96 (d, J = 14.4 Hz, 1H), 2.68−2.62 (m, 1H), 2.19−2.08 (m, 1H), 1.87 (d, J = 10.0 Hz, 1H), 1.76−1.67 (m, 2H), 1.61−1.56 (m, 1H), 1.38−1.31 (m, 2H); ^{13}C NMR (400 MHz, DMSO-d_6): δ 156.6, 149.2, 148.2, 129.7, 125.7, 125.1, 124.9, 124.2, 124.0, 122.8, 115.5, 105.6, 104.7, 103.8, 69.8, 59.8, 57.1, 55.8, 55.3, 33.8, 33.0, 30.4, 29.1, 25.4, 23.9.

*Synthesis of (2S)-2-((2,3-Dimethoxy-11,12,13,14,14a,15-hexahydro-9H-dibenzo[f,h]pyrido[1,2-b]isoquinolin-6-yl)oxy)ethyl 2-Aminopropanoate (**25**).* To a solution of **23** (0.39 g, 0.96 mmol) in dichloromethane (50 mL) were succesively added *N*-Boc-alanine (0.2 g, 1.1 mmol), 1-ethyl-3-(3-(dimethylamino)propyl)carbodiimide hydrochloride (0.37 g, 1.92 mmol), triethyl amine (0.19 g, 1.92 mmol), and DMAP (0.23 g, 1.92 mmol). The mixture was stirred at room temperature for 8 h and was then quenched with suturated ammonium chloride. The organic layler was separated, and the water layer was extracted with dichloromethane three times. The combined organic layer was washed with brine, dried with anhydrous magnesium sulfate, filtered, and concentrated in vacuo. The residue was purified by flash column chromatography on silica gel (dichloromethane:methanol 40:1 as eluent) to give **24** as a light-yellow solid. **24** was dissolved in dichloromethane (30 mL), and trifluoroacetic acid (5 mL) was added. The mixture was stirred at room temperature for 2 h, and saturated sodium bicarbonate was then added. The organic layler was separated, dried with anhydrous magnesium sulfate, filtered, and concentrated in vacuo to give **25** as a yellow-green solid (0.33 g, 72%). mp 204−206 °C; purity 95% in dr 1:3 (HPLC); ^{1}H NMR (400 MHz, $CDCl_3$): δ 7.93 (d, J = 2.0 Hz, 1H), 7.90 (s, 1H), 7.79 (d, J = 8.8 Hz, 1H), 7.25 (s, 1H), 7.19 (dd, J = 8.8 Hz, J = 2.0 Hz, 1H), 4.58 (s, 1H), 4.47 (d, J = 15.6 Hz, 1H), 4.41 (s, 1H), 4.12 (s, 3H), 4.06 (s, 3H), 3.70−3.60 (m, 2H), 3.31 (d, J = 11.2 Hz, 1H), 3.14−3.09 (m, 1H), 2.97−2.90 (m, 1H), 2.47 (s, 1H), 2.38−2.31 (m, 1H), 2.07−2.05 (m, 1H), 1.92−1.72 (m, 5H), 1.63−1.53 (m, 1H), 1.48−1.43 (m, 1H), 1.36 (d, J = 6.8 Hz, 3H); ^{13}C NMR (400 MHz, $CDCl_3$): δ 176.7, 156.3, 149.5, 148.5, 130.2, 126.4, 125.1, 124.7, 124.2, 123.9, 123.4, 115.2, 105.8, 103.8, 66.1, 63.3, 57.6, 56.1, 56.0, 50.1, 34.5, 33.5, 29.7, 25.7, 24.2, 20.8; HRMS (ESI) calcd for $C_{28}H_{35}N_2O_5$ $[M + H]^+$, 479.2546; found, 479.2532.

Cell Lines and Cell Culture. Human gastric adenocarcinoma cell line SGC-7901, hepatocellular carcinoma cell lines BEL-7402, BEL-7404, HuH-7, SK-HEP-1, premyelocytic leukemia cell line HL-60, chronic myelogenous leukemia cell line K-562, renal carcinoma cell line 786-O, colon adenocarcinoma cell line COLO 205, and hepatocyte cell line LO2 were obtained from the cell bank at Shanghai Institute's Cell Resource Center, Chinese Academy of Sciences. Glioblastoma cell line U-118MG, MDR cell subline HL-60/MX2 (Topo II deficient), lung adenocarcinoma cell line A549, breast carcinoma cell lines T-47D, MCF7, MDA-MB-231, and MDA-MB-157, oral epidermoid carcinoma cell line KB, gastric carcinoma cell line KATO III, colorectal adenocarcinoma cell line HCT 116, hepatocellular carcinoma cell lines Hep3B and HepG2, cervical carcinoma cell line HeLa, prostate cancer cell line PC-3, ovarian cancer cell line SKOV-3, pharyngeal carcinoma cell line Detroit 562, B cell lymphoma cell line SU-DHL-6, pancreas adenocarcinoma cell line BxPC-3, and lung fibroblast cell lines MRC-5 and MRC-9 were purchased from American Type Culture Collection. Human rhabdomyosarcoma cell line Rh-30 was a gift from the St. Jude Children's Research Hospital. Human hepatocellular carcinoma cell lines SMMC-7721 and Zip-177 were gifts from the Second Military Medical School (Shanghai, China). Stomach cancer cell line MKN-45 was obtained from the Japanese Foundation of Cancer Research. Adriamycin-selected MDR cell subline K562/ADR was purchased from Nanjing KeyGEN BioTECH Co., Ltd. MDR cell subline KB/VCR was obtained from Zhongshan University of Medical Sciences.

KATO III cells were maintained in IMDM with 20% fetal bovine serum (FBS, Life Technologies). U-118MG, MCF7, HuH-7, SK-HEP-1, and SKOV-3 cells were maintained in DMEM with 10% FBS. PC-3 and A549 cells were maintained in F-12 medium with 10% FBS. MDA-MB-231 and MDA-MB-157 cells were maintained in L15 medium with 10% FBS. HCT 116 cells were maintained in 5A medium with 10% FBS. Hep3B, HepG2, Detroit 562, MRC-5, and MRC-9 cells were maintained in EMEM with 10% FBS. KB and KB/VCR cells were maintained in MEM with 10% FBS. The remaining cells were maintained in RPMI 1640 medium with 10% FBS. IMDM, EMDM, F-12, L15, and 5A media were purchased from Life Technologies Corporation. MEM, DMEM, and RPMI 1640 media were purchased from Corning Corporation. MDA-MB-157 and MDA-MB-231 cells were cultured in a humidified atmosphere of air at 37 °C; other cells were incubated in a humidified atmosphere of 95% air plus 5% CO_2 at 37 °C.

SRB and MTT Assays. The antiproliferative activity of compounds was assessed using an MTT assay with suspended cells (i.e., HL-60, K-562, SU-DHL-6, K562/ADR, and HL-60/MX2 cells) or by an SRB assay with the other adherent cells as previously described.[9] Briefly, cells were seeded in 96-well plates and treated in triplicate with compounds for 72 h. For the MTT assay, 20 μL of MTT solution (5 mg/mL) was added to each well. The plates were further incubated at 37 °C for 4 h, allowing MTT to change into dark-blue formazan crystals, followed by the addition of 100 μL of water-based solubilizing solution (10% SDS, 5% isobutyl alcohol, 10 mM HCl) into each well. For the SRB assay, cells were fixed with 10% ice-cold trichloroacetic acid and stained with 0.4% SRB in 1% acetic acid. The absorbance of each well was measured at 570 nm for the MTT assay or at 540 nm for the SRB assay with a VERSMax plate reader (Molecualr Devices, Sunnyvale, CA) The antiproliferative activity was expressed as IC_{50} values, determined by the four-parameter logistic method. Mean IC_{50} values were obtained from at least three independent experiments.

Cell Proliferation Assay. BEL-7402 cells were seeded in 12-well plates at a density of 1.5×10^4 cells per well and treated in triplicate with a gradient of concentrations of compounds. Cells were then incubated in a IncuCyte ZOOM live cell imaging system (Essen BioScience) for 10 days. This system takes phase-contrast images in real time and automatically calculates the relative phase-contrast area at each time point. The data were retrieved, and proliferation curves were plotted.

Colony Formation Assay. BEL-7402 cells were seeded in 12-well plates at a density of 200 cells per well. Cells were treated in triplicate with compounds for 24 h, and then compounds were removed from the medium by washing twice with PBS. Cells were further incubated in fresh medium for 12 days. Colonies were visualized by staining with SRB, and the number of colonies formed on each plate was quantified by counting stained colonies with a diameter $\geq$ 1 mm.

Cell Cycle Analysis. Treated cells were collected and fixed in 70% ethanol at −20 °C for at least for 1 h. The fixed cells were stained with 50 μg/mL propidium iodide and 10 μg/mL RNase A for 30 min in the dark at room temperature. DNA content was measured with a FACS

DOI: 10.1021/acs.jmedchem.6b01502
J. Med. Chem. XXXX, XXX, XXX−XXX

Calibur flow cytometer (BD Biosciences), and cell cycle distribution was analyzed using ModFit LT software or FlowJo software. For each sample, ≥1.0 × 10^4 cells were analyzed. For cell synchronization, exponentially growing cells were incubated with 0.2 μg/mL aphidicolin (Santa Cruz) for 16 h.

Western Blot Analysis. BEL-7402 cells (1.5 × 10^5) were seeded in 12-well plates and exposed to compounds at the indicated concentrations for various amounts of time. Cells were harvested and subjected standard western blot analysis, using antibodies against γH2AX, p-Chk1 Ser345, or p-Chk2 Thr68 (all from Cell Signaling Technology) or β-actin (Sigma-Aldrich). Relative gray intensity of bands was analyzed with ImageQuant TL software (GE Healthcare Life Sciences).

Apoptosis Assay. Cells undergoing apoptosis were detected using an annexin V−FITC apoptosis detection kit (KeyGEN BioTECH) according to the manufacturer's instructions. Briefly, BEL-7402 cells (3 × 10^5) were seeded in 6-well plates and exposed to compounds at the indicated concentrations for 72 h. Cells were harvested and washed with PBS, resuspended in 100 μL of cold binding buffer with 5 μL of annexin V−FITC and 5 μL of PI, and incubated for 15 min in the dark at room temperature. Annexin V and PI staining were measured with a FACS Calibur flow cytometer (BD Biosciences) and analyzed with FlowJo software.

BrdU Labeling. BEL-7402 cells (3 × 10^5) were seeded in 6-well plates and exposed to compounds at the indicated concentrations for 1 h. Cells were labeled with 10 μM BrdU for 30 min before harvesting. Cells were trypsinized, washed with PBS, and fixed in 70% ethanol at −20 °C for at least 1 h. After fixation, cells were washed with PBS and incubated in 2 N HCl for 20 min. Cells were neutralized with 0.1 M borate buffer for 2 min and incubated with anti-BrdU-FITC (BD Biosciences) and PI for 30 min in the dark at room temperature. Labeled cells were analyzed by flow cytometry and analyzed with FlowJo software.

Trypan Blue Staining. BEL-7402 cells (5 × 10^4) were seeded in 12-well plates and exposed to compounds at the indicated concentrations for 72 h. Cells were trypsinized and stained with 0.4% Trypan blue solution (Life Technology) at a 9:1 dilution for 3 min and were then loaded into a hemocytometer to count the unstained (viable) and stained (necrotic) cells separately.

Statistical Analysis. All experiments were repeated independently three times. Data are presented as the mean ± SD. Significance was analyzed with Student's t test. Results were considered statistically significant at $p < 0.05$ (notation: *, $p < 0.05$; **, $p < 0.01$).

■ ASSOCIATED CONTENT

Supporting Information

The Supporting Information is available free of charge on the ACS Publications website at DOI: 10.1021/acs.jmedchem.6b01502.

^{1}H and ^{13}C NMR spectra of **2-rac**; DEPT, CH-COSY, and HH-COSY of **2-R**; ^{1}H NMR, ^{13}C NMR, HRMS, and HPLC spectra of compounds **1** and **7**−**25**; procedure for primary neuronal cell culture and treatment; effects of **2-R** and **21-R** on the viability of rat primary neurons (Table S1); and effects of compounds **1** and **2-R** on the expression of P-gp (Figure S1) (PDF)

Molecular formula strings and associated biological data (CSV)

■ AUTHOR INFORMATION

Corresponding Authors

*(L.-h.M.) Phone: 86-21-50806722. Fax: 86-21-50806722. E-mail: lhmeng@simm.ac.cn.

*(Q.W.) Phone: 86-22-23503952. Fax: 86-22-23503952. E-mail: wangqm@nankai.edu.cn.

ORCID

Qingmin Wang: 0000-0002-6062-3766

Author Contributions

§Y.L., L.Q., C.M., and J.S. contributed equally to this work.

Notes

The authors declare no competing financial interest.

■ ACKNOWLEDGMENTS

We are grateful to the National Natural Science Foundation of China (21421062, 21372131, 21672117 and 81321092), the Specialized Research Fund for the Doctoral Program of Higher Education (20130031110017) and the Tianjin Natural Science Foundation (16JCZDJC32400) for generous financial support for our programs. We would like to Thank Huan Wang from Shanghai Institute of Materia Medica for the help in the cytotoxic assay of rat neurons.

■ ABBREVIATION USED

ADR, adriamycin; BCRP, breast cancer resistance protein; BrdU, 5-bromodeoxyuridine; CHK1, checkpoint kinase 1; CHK2, checkpoint kinase 2; CPT, camptothecin; DMSO, dimethyl sulfoxide; DMAP, 4-dimethylaminopyridine; EDCI, (3-(dimethylamino)propyl)ethyl carbodiimide hydrochloride; IC_{50}, 50% inhibitory concentration; MDR, multidrug resistance; MTT, 3-(4,5-dimethylthiazol-2-yl)-2,5-diphenyltetrazolium; NVT, novantrone; PBS, phosphate buffered saline; P-gp, P-glycoprotein; SRB, sulforhodamine B; VCR, vincristine

■ REFERENCES

(1) Ratnagiriswaran, A.; Venkatachalam, K. The chemical examination of Tylophora asthmatica and isolation of the alkaloids tylophorine and tylophorinine. *Indian. J. Med. Res.* **1935**, *22*, 433−441.

(2) Gellert, E.; Rudzats, R. The antileukemia activity of Tylocrebrine. *J. Med. Chem.* **1964**, *7*, 361−362.

(3) Cassady, J. M.; Douros, J. D. *Anticancer Agents Based on Natural Product Models*; Academic Press: New York, 1980.

(4) Ali, M.; Ansari, S. H.; Qadry, J. S. Rare phenanthroindolizidine alkaloids and a substituted phenanthrene, tyloindane, from Tylophora-Indica. *J. Nat. Prod.* **1991**, *54*, 1271−1278.

(5) Gao, W.; Lam, W.; Zhong, S.; Kaczmarek, C.; Baker, D. C.; Cheng, Y. C. Novel mode of action of tylophorine analogs as antitumor compounds. *Cancer Res.* **2004**, *64*, 678−688.

(6) Shiah, H. S.; Gao, W.; Baker, D. C.; Cheng, Y. C. Inhibition of cell growth and nuclear factor-kappaB activity in pancreatic cancer cell lines by a tylophorine analogue, DCB-3503. *Mol. Cancer Ther.* **2006**, *5*, 2484−2493.

(7) Ikeda, T.; Yaegashi, T.; Matsuzaki, T.; Hashimoto, S.; Sawada, S. Asymmetric synthesis of phenanthroindolizidine alkaloids with hydroxyl group at the C14 position and evaluation of their antitumor activities. *Bioorg. Med. Chem. Lett.* **2011**, *21*, 342−345.

(8) Wu, C. M.; Yang, C. W.; Lee, Y. Z.; Chuang, T. H.; Wu, P. L.; Chao, Y. S.; Lee, S. J. Tylophorine arrests carcinoma cells at G1 phase by downregulating cyclin A2 expression. *Biochem. Biophys. Res. Commun.* **2009**, *386*, 140−145.

(9) Wang, Z.; Wu, M.; Wang, Y.; Li, Z.; Wang, L.; Han, G.; Chen, F.; Liu, Y.; Wang, K.; Zhang, A.; Meng, L.; Wang, Q. Synthesis and SAR studies of phenanthroindolizidine and phenanthroquinolizidine alkaloids as potent anti-tumor agents. *Eur. J. Med. Chem.* **2012**, *51*, 250−258.

(10) Staerk, D.; Lykkeberg, A. K.; Christensen, J.; Budnik, B. A.; Abe, F.; Jaroszewski, J. W. In vitro cytotoxic activity of phenanthroindolizidine alkaloids from Cynanchum vincetoxicum and Tylophora tanakae against drug-sensitive and multidrug-resistant cancer cells. *J. Nat. Prod.* **2002**, *65*, 1299−1302.

DOI: 10.1021/acs.jmedchem.6b01502
J. Med. Chem. XXXX, XXX, XXX−XXX

(11) Staerk, D.; Christensen, J.; Lemmich, E.; Duus, J. O.; Olsen, C. E.; Jaroszewski, J. W. Cytotoxic activity of some phenanthroindolizidine N-oxide alkaloids from Cynanchum vincetoxicum. *J. Nat. Prod.* **2000**, *63*, 1584−1586.
(12) Chemler, S. R. Phenanthroindolizidines and phenanthroquinolizidines: promising alkaloids for anti-cancer therapy. *Curr. Bioact. Compd.* **2009**, *5*, 2−19.
(13) Donaldson, G. R.; Atkinson, M. R.; Murray, A. W. Inhibition of protein synthesis in Ehrlich ascites-tumour cells by the phenanthrene alkaloids tylophorine, tylocrebrine and cryptopleurine. *Biochem. Biophys. Res. Commun.* **1968**, *31*, 104−109.
(14) Huang, M. T.; Grollman, A. P. Mode of action of tylocrebrine: effects on protein and nucleic acid synthesis. *Mol. Pharmacol.* **1972**, *8*, 538−550.
(15) Rao, K. N.; Bhattacharya, R. K.; Venkatachalam, S. R. Inhibition of thymidylate synthase and cell growth by the phenanthroindolizidine alkaloids pergularinine and tylophorinidine. *Chem.-Biol. Interact.* **1997**, *106*, 201−212.
(16) Rao, K. N.; Venkatachalam, S. R. Dihydrofolate reductase and cell growth activity inhibition by the beta-carboline-benzoquinolizidine plant alkaloid deoxytubulosine from Alangium lamarckii: its potential as an antimicrobial and anticancer agent. *Bioorg. Med. Chem.* **1999**, *7*, 1105−1110.
(17) Liu, Z. J.; Lv, H. N.; Li, H. Y.; Zhang, Y.; Zhang, H. J.; Su, F. Q.; Si, Y. K.; Yu, S. S.; Chen, X. G. Anticancer effect and neurotoxicity of S-(+)-deoxytylophorinidine, a new phenanthroindolizidine alkaloid that interacts with nucleic acids. *J. Asian Nat. Prod. Res.* **2011**, *13*, 400−408.
(18) Ueno, S.; Yamazaki, R.; Ikeda, T.; Yaegashi, T.; Matsuzaki, T. Antitumor effect of a novel phenanthroindolizidine alkaloid derivative through inhibition of protein synthesis. *Anticancer Res.* **2014**, *34*, 3391−3397.
(19) Gao, W.; Bussom, S.; Grill, S. P.; Gullen, E. A.; Hu, Y. C.; Huang, X.; Zhong, S.; Kaczmarek, C.; Gutierrez, J.; Francis, S.; Baker, D. C.; Yu, S.; Cheng, Y. C. Structure-activity studies of phenanthroindolizidine alkaloids as potential antitumor agents. *Bioorg. Med. Chem. Lett.* **2007**, *17*, 4338−4342.
(20) Yang, C. W.; Lee, Y. Z.; Hsu, H. Y.; Wu, C. M.; Chang, H. Y.; Chao, Y. S.; Lee, S. J. c-Jun-mediated anticancer mechanisms of tylophorine. *Carcinogenesis* **2013**, *34*, 1304−1314.
(21) Cai, X. F.; Jin, X.; Lee, D.; Yang, Y. T.; Lee, K.; Hong, Y. S.; Lee, J. H.; Lee, J. J. Phenanthroquinolizidine alkaloids from the roots of Boehmeria pannosa potently inhibit hypoxia-inducible factor-1 in AGS human gastric cancer cells. *J. Nat. Prod.* **2006**, *69*, 1095−1097.
(22) de Fatima Pereira, M.; Rochais, C.; Dallemagne, P. Recent advances in phenanthroindolizidine and phenanthroquinolizidine derivatives with anticancer activities. *Anti-Cancer Agents Med. Chem.* **2015**, *15*, 1080−1091.
(23) Wang, Z.; Feng, A.; Cui, M.; Liu, Y.; Wang, L.; Wang, Q. First discovery and stucture-activity relationship study of phenanthroquinolizidines as novel antiviral agents against tobacco mosaic virus (TMV). *PLoS One* **2012**, *7*, e52933.
(24) Lieby-Muller, F.; Marion, F.; Schmitt, P.; Annereau, J. P.; Kruczynski, A.; Guilbaud, N.; Bailly, C. Synthesis and biological evaluation of (−)-6-O-desmethylcryptopleurine and analogs. *Bioorg. Med. Chem. Lett.* **2015**, *25*, 184−187.
(25) Wang, Q.; Meng, C.; Liu, Y.; Wang, C. Method for preparation of phenanthroquinolizidine alkaloid and its 6-position derivatization product, and their application as antiviral and anticancer agents. Faming Zhuanli Shenqing CN 105884761 A, 2016.
(26) Wang, Z. W.; Wang, Q. M. Highly efficient synthesis of phenanthroquinolizidine alkaloids via Parham-type cycliacylation. *Tetrahedron Lett.* **2010**, *51*, 1377−1379.
(27) Wang, Z. W.; Wang, L.; Wang, Q. M. First and efficient synthesis of 14-aminophenanthroindolizidine alkaloids. *Synthesis* **2011**, *2011*, 979−983.
(28) Johnston, S. T.; Shah, E. T.; Chopin, L. K.; Sean McElwain, D. L.; Simpson, M. J. Estimating cell diffusivity and cell proliferation rate by interpreting IncuCyte ZOOM assay data using the Fisher-Kolmogorov model. *BMC Syst. Biol.* **2015**, *9*, 38.
(29) Huang, M.; Miao, Z. H.; Zhu, H.; Cai, Y. J.; Lu, W.; Ding, J. Chk1 and Chk2 are differentially involved in homologous recombination repair and cell cycle arrest in response to DNA double-strand breaks induced by camptothecins. *Mol. Cancer Ther.* **2008**, *7*, 1440−1449.

DOI: 10.1021/acs.jmedchem.6b01502
J. Med. Chem. XXXX, XXX, XXX−XXX